Temporal changes in MSL air pressure and associated atmospheric thermal anomalies, especially in the stratosphere.

B J Burton.

Abstract.

The geopotential at a point at any level in the atmosphere depends on just two factors: 1.) the geopotential at some higher level directly above. 2) the intervening temperature. For fixed pressure levels, the distance between them, the thickness of the layer, is directly proportional to the mean temperature of the layer. During developments in the troposphere, a level can be found higher in the atmosphere where the geopotential field remains undisturbed. It then follows that, in an atmosphere near geostrophic balance, any change in geopotential, and wind field, which are observed below the undisturbed level, can only result from changes in the thermal field in the intervening layer. The relationship of thermal anomalies in the stratosphere to developments in the troposphere is examined, and case histories are presented using actual data, which clearly demonstrate the importance of this relationship. A better understanding of the interaction of the thermal field with the atmosphere below, and how developments near the upper troposphere are largely governed by changes in the thermal field in the overlying lower stratosphere, will help meteorologists to understand the essential thermodynamic feedback mechanisms that operate in this region of the atmosphere. Mention is also made of the link between the upper stratosphere and troposphere via downward propagation. The part played by vorticity, especially important in the upper troposphere in relation to jet-streams and their dynamics, is examined.

Introduction.

In an article, Tropopause Undulations and the Development of Extratropical Cyclones, Paul Hirschberg and J Michael Fritsh, (1991), subsequently referred to as HR in this article, put forward a perspective of the upper troposphere/lower stratosphere much in accord with the findings discussed in this article.

During the late 1980s and early 1990s, case histories were assembled in order to examine the relationship between thermal changes in the upper atmosphere and the changes in the pressure pattern at lower levels. It is evident that in order to produce the observed pressure changes at the surface of the earth during cyclonic/anticyclonic development, the net thermal changes in the

atmosphere above must be inversely related to those commonly observed in the troposphere alone. In the absence of any other effects, mass ascent, that produces cooling in the troposphere, and descent, which produces warming, will tend to raise the surface pressure near a cyclonic development, and lower it near a building anticyclone, the opposite effect to the one observed, and not a tenable scenario. There must, then, have been thermal changes in the atmospheric column over developing cyclones or anticyclones in a part of the atmosphere which lies above the troposphere, which are sufficient to more than offset the tropospheric thermal tendency. In the mid-latitude cases examined, the expected thermal changes were found in the stratosphere, and were usually most marked in the lower part of it.

Data has been assembled from both real atmospheric soundings, and from model forecast runs using the Meteorological Office routine coarse and fine mesh output (pre 1991), during interesting periods, usually of mid-latitude cyclonic development, although the model constraints imposed by an artificial upper boundary in the stratosphere limit their uppermost useful level to about 100 hPa in this type of investigation. In the case histories used here, only real data has been used, with model output being introduced only for comparative purposes, to obtain a general overview of the development, and for illustration in the discussion section.

As the number of cases examined increased, it was evident that the pressure pattern, and therefore the wind field, at upper tropospheric levels, is closely tied to the thermal pattern in the lower and mid-stratosphere. Contour ridges/troughs in the upper troposphere are always overlain by cold/warm thermal anomalies in the atmosphere above. It also became evident that there must be feedback paths between the development of the thermal pattern in the lower stratosphere, and changes in vorticity in the upper troposphere.

In this paper, five mid/latitude northern hemisphere case histories are presented, drawn from the many studied, which will illustrate the active role played by the atmosphere above the troposphere in shaping tropospheric and surface developments. The main method used to study the atmosphere in these cases is through the concept of layer thickness, which is directly proportional to layer mean temperature. As HF note in their paper, in the upper atmosphere a level is usually reached where changes occur only slowly, and proceed independently of events below them. This has been found to be true for the majority of cases looked at here, and has led to an alternative, though perhaps not new, view of how the atmosphere works.

Thickness and Pressure.

It is well established that the air pressure at a point on the surface of the earth is a result of gravity acting on all the air molecules in a vertical column above that point. It then follows that the air pressure at any point and altitude in the atmosphere depends on the weight or mass of air above that point.

The pressure at a height z above a level where the pressure is p(0) can be determined from :

$$p(z) = p(0) \exp(-gz/RT) \quad \text{hPa} \qquad (1)$$

where g = acceleration due to gravity, 9.80665

R = gas constant for dry air (per kg) , 287

T = Mean temperature between the pressure surfaces, Deg K.

Eq 1 is sometimes called the altimeter equation. However, it is usually more convenient to work in surfaces of constant pressure in the atmosphere, and eq 1 can be written in the form:

$$Z' = Z_U - Z_L = RT/g * \ln(p_U/p_L) \quad \text{m} \qquad (2)$$

Where Z' is the thickness between pressure levels p_L and p_U, and where p_L is the pressure at the base of the layer and p_U at the top.

From eq 2 we see that the thickness of a layer is proportional to the mean temperature of the layer. This is true where ever the pressure surfaces are located in the atmosphere, at least up to 80 km or so, after which the molecular constituents may cease to be well mixed and uniform, and R ceases to be constant.

The change in thickness in a layer bounded by fixed pressure surfaces, $\Delta Z'$, in distance and/or time, is also directly proportional to the change in mean temperature in the layer.

$$\Delta Z' = k\Delta T \quad \text{m} \qquad (3)$$

Where $k = R/g*\ln(p_U/p_L)$

From the above we see that changes in geopotential height on any pressure surface come about as the result of the mean temperature in a column extending above that pressure surface. This can be put in another way, the changes in pressure at any fixed altitude in the atmosphere come about due

to changes in the mean temperature in a column extending above that altitude. If that altitude is 0, as it is at the earth's surface, then changes in surface pressure are proportional to changes in the mean temperature of the column of the entire atmosphere above. Importantly, eq 3 tells us that for any atmospheric layer where the ratio of p_U to p_L is the same, the change in thickness that accompanies a change in mean temperature of the layer will also be the same. Thus, the change in pressure at the base of a layer for a given change in temperature in that layer will be the same if the layer is bounded by the pressures of 1000 and 300 hPa, often the entire troposphere, as with one bounded by 100 and 30 hPa, a small portion of the lower stratosphere.

The concept that the pressure at any point in the atmosphere depends on the mean temperature of a column extending vertically upwards from that point is not new. Yet it seems that it is sometimes missed by some investigators who attempt to show that upper tropospheric synoptic scale developments are initiated by changes going on at lower levels. This is rarely, if ever, found to be the case in practice, and on the contrary developments in the lower troposphere usually follow from forcing applied from above, and developments at higher levels follow from forcing applied from above that level.

It could be argued that changes in thickness in a layer might not only lead to changes in pressure at the base of the layer, but also to changes in pressure at the top. However, observation on scales bordering the synoptic in the troposphere seems not to support that hypothesis, although on very large scales, both temporal and spatial, evidence from the behaviour of the mesosphere to the annual cycle of temperature in the stratosphere suggests that pressure at the stratopause increases as the temperature in the layers below increase, and vice versa. Here the dominant effect seems to be the expansion of a very large volume, with the associated cooling due to adiabatic expansion in the mesosphere being unchecked by photochemical thermal changes, as are proceeding in the layers below. It should be noted here that the pressure change due to the annual cycle falls to near zero near the mesopause, between 80 and 90 km altitude.

To investigate if, indeed, changes in thickness in a layer cause the pressure at the base and not the top to change, the two examples that follow make use of the data also used in an article by Burton (1993) which discussed the same topic.

Example 1. Surface pressure changes due to diurnal boundary layer heating, Southern England, 11 May 1980.

Using surface observations and routine radio-sonde ascents, it was found that the diurnal fall in surface pressure at inland sites compared with that at coastal ones was exactly that expected from the observed changes in geostrophic thickness in the boundary layer. A strong onshore flow over the

coastal sites brought boundary layer air modified by its passage over a cool sea, and with a subsidence inversion near 900 hPa that confined the inland diurnal heating to below that level. At the coastal stations, screen temperatures remain near 10° C throughout 24 hours, while inland a diurnal screen temperature range of near 17° C was observed. From the 0000 UTC and 1200 UTC routine radio-sonde ascents for Hemsby (52.7N 1.7E) near the windward North Sea coast of East Anglia, and Crawley, (51.2N 0.2W), 50km inland from the windward coast, values of geopotential thickness for sub-layers in the boundary layer between 850 hPa and 1020 hPa were calculated. The 12 hour thickness change between 00 and 12 GMT at both stations is shown in Table 1.

MSL pressure changes over southern England for the period 0600 UTC to 1200 UTC were:
Mean coastal = -1.1 hPa, mean inland = -2.7 hPa. Difference inland minus coastal, -1.6 hPa

MSL pressure change in 12 hours, 0000 UTC to 1200 UTC were:
Hemsby (coastal) = -2.4 hPa Crawley (inland) = -5.4 hPa Difference -3.0 hPa

Table 1 Thickness change in gpm at Hemsby and Crawley over selected constant pressure levels in the boundary layer, between 0000 UTC and 1200 UTC on 11 May 1980 and the resulting change in surface MSL pressure.

Layer hPa	Hemsby	Crawley	Geopotential difference
850/900	0 m	+1 m	-6 m
900/940	-1	+3	-10
940/980	-2	+3	-15
980/1020	-2	+8	-25
Total 850/1020	-5	+15	
Background change in 850 hpa geopotential	-24	-29	
Total change in 1020 hPa height	-19	-44	
Equivalent change in MSL pressure	-2.3 hPa	-5.3 hPa	-3.0 hPa
Reported change, surface observations	-2.4 hPa	-5.4 hPa	-3.0 hPa

Example 2. Tethered balloon soundings taken at Cardington, England (52.1N 0.4W) at 1000 UTC and 1400 UTC on 11th May 1980, during which 4 hours time interval the boundary layer mean temperature increased by about 2° C. There was a capping inversion near 900 hPa with subsided air above. The air was very dry, with a humidity mixing ratio of 3 to 5 g/kg in the boundary layer, decreasing to 1 to 2 g/kg above the inversion.

Table 2.

Layer hPa	4 hour thickness change, m
900 to 920	+0.7
920 to 940	+1.2
940 to 960	+1.2
960 to 980	+0.9
980 to 1000	+1.0
1000 to 1020	+1.3
Total	+6.3

a) Background change in 850 hPa geopotential = -14.5 m

b) MSLP change due to background change at 850 hPa = -1.7 hPa

c) MSLP change due to boundary layer thickness change = -0.7 hPa

d) Total expected change in MSLP from ascent data = -2.4 hPa

e) Recorded MSLP change = -2.5 hPa

The two examples above show that the diabatic boundary layer heating reduces the surface pressure exclusively, and does not change the pressure at the top of the boundary layer. In both examples, the change in MSLP at inland stations is entirely accounted for by the rise in thickness in the boundary layer. In example 1, after allowing for the background synoptic change at 850 mbar, the 12 hour geopotential change at 900 hPa is only +/- 1 gpm.

Returning to a wider perspective, when considering the possible effects of thickness changes in the atmosphere generally, it is important to appreciate the impact that differing temperature lapse rates can have. Dynamic effects which lead to vertical motion in the atmosphere can also lead to changes in layer mean temperature as a result of adiabatic adjustment. The sole exception is when the temperature lapse rate is already at the dry adiabatic rate, i.e. when the change of potential temperature with height is zero, then any vertical displacement in unsaturated conditions will have no effect on the layer mean temperature. In general, the further that the lapse rate decreases from the dry adiabatic rate, (rate of change of potential temperature with height is >

zero), the greater the change in layer thickness for a given vertical displacement. Sources of layer thickness change associated with diabatic processes include radiation heating and cooling, including photochemical changes due to radiation in the stratosphere, change of state of the water fraction (troposphere only), and turbulent exchanges at the top and/or base of the layer. As the ambient lapse rate is generally closer to adiabatic in the troposphere than in the stratosphere, then vertical displacements of equal magnitude will lead to greater changes in layer thickness in the stratosphere than in the troposphere.

Vorticity.

Knowledge of vorticity, or spin, of the air about a vertical axis, and changes in vorticity along the flow, can give a useful insight into dynamically induced vertical motions, which in turn have a fundamental influence on the thermal evolution of atmospheric layers, especially in the stratosphere, and can lead to better understanding of how thermal anomalies can be generated and maintained. Relative vorticity, ζ, may be defined as follows:

$$\zeta = v/r - \Delta v/\Delta n \qquad 4.$$

Where v is the horizontal air velocity, r is the radius of curvature of the flow, and $\Delta v/\Delta n$ is the cross flow shear in a direction normal and to the left to the flow.

Because the earth and atmosphere are rotating, even if the air is stationary relative to the earth's surface, it will share a component of the earth's vorticity about the local vertical.

The earth's vorticity, f, may be defined as follows:

$$f = 2*\Omega*\sin\phi \qquad 5.$$

Where Ω is the earth's angular velocity, 7.29×10^{-5} rad s^{-1} and ϕ is the latitude.

$$\text{Absolute vorticity } \zeta_a = \zeta + f \qquad 6.$$

The changes in vorticity along the flow for a horizontal circular area of particles causes the area to change, decreasing vorticity leading to an increase in area, and vice-versa. But if a small column is considered, whose circumference is a vertical extension of that of the area, then changes in the horizontal area will be accompanied by compensating changes in the height of the column,

such that the volume tends to remain nearly constant. Thus for any atmospheric column moving with the flow, horizontal shrinkage/expansion, associated with increasing/decreasing vorticity is always accompanied by vertical stretching/contraction.

Vorticity can be related to the length of a column defined by the difference between the pressure at the top and base of the column, Δp, such that:

$$\zeta_a = k * \Delta p \qquad 7.$$

and where k is a constant.

If a conservative property of the atmosphere is considered, e.g. potential temperature, which is conserved during adiabatic motion in the lower stratosphere, at least on relatively short time scales, equation 7 shows that the distance separating adjacent pairs of potential temperature surfaces will be directly proportional to the absolute vorticity. With the normally steep increase in potential temperature in the lower stratosphere, changes in vorticity along the flow will change the pressure at which given potential temperature isentropes are found, and this change will be accompanied by a change in the thickness of the layer.

Changes in thickness, then, are linked to changes in the absolute vorticity experienced by discreet entities of air as they flow through a particular pattern. Horizontal shear and curvature contribute to vorticity, equation 4, and both terms are have the potential to be greatest where the flow is strongest. It is not surprising, then, to find a maxima in horizontal vorticity gradient near the level of the maximum wind, usually in the upper troposphere. It is commonly found that horizontal vorticity gradients decrease away from this level, both upwards and downwards, but in some situations may increase again higher in the atmosphere, particularly in the vicinity of the polar night jet. The lower stratosphere is thus a region where the amplitude of vorticity change experienced by the columns of particles is decreasing with increasing altitude, but where high values may also be found. It is, then, not surprising to find that this region of the atmosphere is dynamically very active and can contain appreciable vertical motion, especially in the presence of jet-stream flow in the upper troposphere.

Thickness Budget.

From equation 2, the geopotential, Z_L , at pressure level p_L , can be found simply from a knowledge of the geopotential at some higher level, Z_U, p_U, so that:

$$Z_L = Z_U - Z' \quad m \qquad 8.$$

where Z' is the thickness of the layer.

Any change in the lower geopotential, either spatially or temporally, can only occur as a result of a change in the geopotential at some higher level, and/or a change in the mean temperature, and thus the thickness, of the layer.

So that changes in the lower geopotential, $\Delta Z_{L,}$ will be the result of:

$$\Delta Z_L = Z_{U-} \Sigma^{pu}_{pl} \Delta Z' \quad m \qquad 9.$$

where, in this case, Z_U can be at an undisturbed level where vorticity changes are small or nil.

The link between thickness and layer mean temperature can be used to advantage when investigating the behaviour of the atmosphere in relation to developments at the earth's surface by using the simple thickness budget method. This involves relating changes in thickness over selected layers of the atmosphere directly to changes in surface pressure. Layer thickness is readily obtained from routine upper air reports, and from model output on standard isobaric surfaces. Using this method as a diagnostic tool has the advantage that it is sensitive to relatively small changes in layer mean temperature, and of showing the contribution being made by different layers of the atmosphere to surface developments. Using model output it is possible to obtain thickness budgets in a semi Lagrangian frame, though with reliability at present (1995) only up to about 100 hPa. Using radio-sonde data it is possible to explore at least to 30 hPa in many cases, and sometimes to 10 hPa, but of course only over a fixed location.

The thickness budget concept evolved when it became evident that for most of the time, on a day-to-day basis, a level in the atmosphere could be found which was undisturbed by any changes going on below, and this level was often located in the stratosphere between 50 and 100 hPa, well within the reach of routine soundings. It was noticed that during disturbed or active periods in the upper troposphere and lower stratosphere, the amplitude of the disturbance invariably diminished upward from the near the tropopause. Some cyclonic events were found which indicated that vertically propagating waves originating in the troposphere were apparently being felt at levels at least as high as 30 hPa, but these were rather an exception, and tended to occur at later stages in the development, and in may mid-latitude cases studied, changes at and above 100 hPa were small, and as found by HF, almost vanish by 50 hPa.

This is important, for if there is an upper undisturbed level, equation 9 shows that any changes in geopotential at any level vertically below the undisturbed level, can only occur if there is a change in thickness in the intervening layer, and cannot occur as a result of thickness changes below that lower level. Also, if it is assumed that the atmosphere is close to geostrophic balance, then any change in geopotential will be numerically equal to, but of the opposite sign from, the total thickness change in the layers vertically above, up to the undisturbed level.

In terms of surface pressure, which for practical purposes can be equated to the geopotential of the 1000 hPa surface, it will owe its current value to the geopotential at some upper level vertically above, minus the total thickness of the intervening atmosphere. Once again, if the upper level is chosen such that it is undisturbed, then changes in surface geopotential are numerically equal to, but of the opposite sign from, changes in total thickness between the undisturbed level vertically above, and the surface, (equation 9). As thickness is directly proportional to mean temperature alone, all geostrophic changes in surface pressure occur as a result of changes in temperature in the overlying atmosphere.

Looking now at the geopotential field at 300 hPa, a level usually near the top of the mid-latitude troposphere and one where the dynamics often drive tropospheric developments. The shape and spacing of the contours of geopotential will determine the local wind field, and the associated vorticity. In the previous paragraph, it was shown that the geopotential field at any level in the atmosphere is determined by that at some higher level vertically above, minus the intervening thickness field. If the higher level is an undisturbed level, then any changes in the shape and strength of the 300 hPa flow will have to be accompanied by changes in the thermal field between the upper undisturbed level and 300 hPa. Associated changes in the strength and direction of the thermal wind in that layer must then result in changes in the strength and direction of the flow at 300 hPa.

To give a simple example in a typical mid-latitude situation, Figures 1a to d (below) show the contrasting types of flow which will result at some lower level from a steady unchanging uniform flow of 240 degrees 40 knots at some upper level, having a warm or cold thermal anomaly in the intervening layer, such as may commonly be seen in the lower stratosphere. Fig1a shows the warm anomaly case and the resulting wind field at the lower level is shown in Fig1b using standard wind arrows, where the strength is in knots. Fig1c shows the cold anomaly case, and this produces a robust anticyclonic circulation in Fig 1d in place of the cyclonic jet in Fig1b. The diagram is not drawn to scale, but the hypothetical thermal winds used in the calculation of the wind field in Fig1b and Fig1d are shown in Table 3.

Table 3. Layer thermal winds used to calculate the lower level winds shown in Figs 1b and 1d, assuming a constant upper level wind of 240/40 kn. Directions in degrees from north, speed knots

Position as shown in Fig1	Warm anomaly case	Cold anomaly case
A	240 / 30	060 / 30
B	290 / 40	110 / 40
C	010 / 90	190 / 90
D	060 / 100	240 / 100
E	080 / 100	260 / 100
F	110 / 70	290 / 70
G	340 / 10	160 / 10

Figure 1. Schematic diagram showing the effect on the flow at lower level when there is a uniform south-westerly gradient of 240° 40 kn, (geopotential contours, solid) at an upper level, and where there is a warm or cold thermal anomaly in the intervening layer, (geopotential thickness

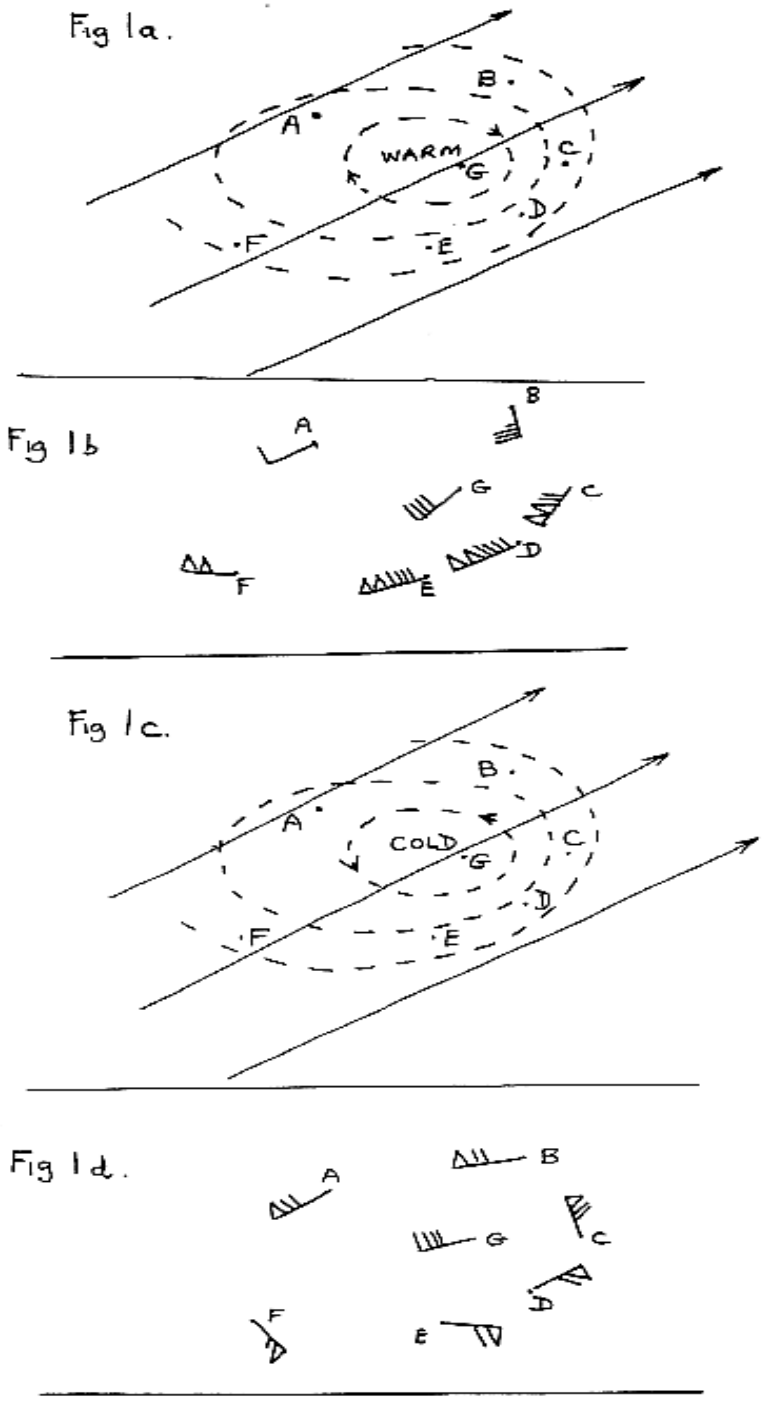

contours, dashed). The wind arrows plotted, (normal convection, in knots), are the resultant wind at the lower level at points marked A to G. Figs 1a and 1b show the warm thermal anomaly case. Figs1c and 1d show the cold thermal anomaly case. Winds below a warm anomaly will have a cyclonic distribution, and below a cold anomaly will have an anticyclonic one.

Before moving on to individual case histories, it is worth repeating the basic premise, as it would appear to be essential to understanding how different parts of the atmosphere interact.

In an atmosphere near geostrophic balance, then at any time and at any level, the pressure pattern and wind field are the result of the pressure pattern and wind field at some higher level, modified by the intervening thermal field.

Case Histories.

Case 1. The record low pressure recorded over southern England on 25th February 1989.

On that day, the pressure fell below 955 hPa over much of southern England, with a value of 952.4 hPa recorded at Wokingham, Berkshire, UK, their lowest pressure for more than 130 years, (For a full description of the event, see Burt 1989.) The centre of the surface low tracked eastwards along the English Channel, with a central pressure of 949 hPa analysed at 1500 UTC. The thermal disposition of the atmosphere in the vicinity of the low was examined using routine radio-sonde ascents released from Crawley in southeast England, (station 03774), during the period 24th February at 0000 UTC to 27th February at 0000 UTC. Ascents were made every 12 hours, and Table 4a shows the partial thickness for selected layers between fixed pressure levels, up to 10 hPa where available. Missing values in the 10 to 100 hPa layer have been estimated using interpolated values at 30 hPa, and these estimated values are shown in parenthesis in Table 4a. Table 4b lists the thickness budget over 12 hour periods for the same station.

Table 4a. Partial thickness, gpdam, for selected atmospheric layers over Crawley, 24th to 27th February 1989, and the MSLP (hPa) at the time of launch of the sounding.

Layer hPa	24/00	24/12	25/00	25/12	26/00	26/12	27/00
10 to 30	722	-	-	-	-	752	760
30 to 100	798	(798)	792	(786)	785	781	766
100 to 300	705	701	711	712	705	695	687
300to 1000	875	879	874	875	873	864	866
1000 ht	-6	-16	-25	-34	-37	-37	-25
MSLP	993	981	970	959	955	967	970

Table 4b. Thickness budget over Crawley, gpdam, 12 hour intervals ending at the time shown.

Layer hPa	24/12	25/00	25/12	26/00	26/12	27/00	48 hours to 26/00
Above 30	+10	+10	+13	+13	+14	+18	+46
30-100	0	-6	-6	-1	-4	-15	-13
100-300	-4	+10	+1	-7	-10	-8	0
300-1000	+4	-5	+1	-2	-9	+2	-2
Net	+10	+9	+9	+3	-9	-3	+31
Change in MSLP hPa	-12	-11	-11	-4	+12	+3	-38

From Tables 4a and 4b it is evident that changes in tropospheric thickness played little part in this rare event. In the two days prior to the lowest pressure, and during which the surface pressure over Crawley fell by 38 hPa, there was net modest cooling of 2 gpdam in the tropospheric layer 300 to 1000 hPa. Even in the lower stratosphere, between 100 and 300 hPa, there is evidence for the passage of a warm anomaly near 1200 UTC on the 25th, for the two day period when the surface pressure was falling, the net change was zero. Higher in the stratosphere, in the 30 to 100 hPa layer, over the same period there was a net fall in thickness of 13 gpdam. These thermal changes, taken on their own, would have caused the surface pressure to rise by nearly 20 hPa. It is the atmosphere above 30 hPa to which we must look for the cause of the prolonged fall in surface pressure which culminated in the record low value being reached. Above 30 hPa, the thickness increased by a notable 46 gpdam in 2 days, and continued increasing right up to the end of the period studied, by which time, just 24 hours later, it had increased by a further 32 gpdam. After 26th 0000 UTC, cold advection in the troposphere coupled with increased cooling in the lower to mid-stratosphere, lifted the surface pressure somewhat by 0000 UTC on the 27th.

Winds measured on the radio-sonde ascents were examined to ascertain the magnitude and sign of the thermal advection in the stratosphere. In the 10 to 30 hPa layer, although the wind at 10 hPa was only available on 3 ascents out of 7, the 24th at 0000 UTC, 26th at 1200 UTC and 27th at 0000 UTC, each ascent showed cold advection in this layer with rates between -10 and -30 m/hr. Despite this substantial cold advection, thickness actually increased by 38 gpdam over the period. Only strong and continuous dynamic descent can explain such a sustained rise in thickness in the face of steady cold advection. Large displacements at these levels are commonly observed during stratospheric warming events, of which this would seem to have been an example.

Taking a wider view of events, at 300 hPa a vortex was located near 70N over Greenland at 12 UTC on the 24th. South of this lay a broad and very strong WNW jet, with speeds in excess of 100 m/s. On the northen periphery of the jet a short wave trough could be detected near 40W. A slow moving long-wave trough lay from just west of Scotland to northern Africa at about 5E. Over the 35 hours up to 00 UTC on the 26th, the vortex tracked SE to be located over the North Sea near 55N. The short-wave trough initially ran very quickly east, eventually slowing and amplifying in the left exit of the jet, extending from central England to the Mediterranean. The long-wave trough, almost stationary for the first 12 hours, split into two, with the northern part rotating northwards ahead of the advancing vortex, and the southern part relaxing gently eastwards.

The timing and track of the surface low over the English Channel was linked closely with that of the short-wave trough, itself being maintained by a warm anomaly in the lower stratosphere, and which showed a peak in the 100 to 300 hPa thickness of 712 gpdam near 12 UTC on the 25th, over

Crawley (Table 4). This peak was about 3 hours before the record minimum surface pressure recorded nearby. The SE movement of the 300 hPa vortex probably reflected the movement of the stratospheric winter vortex as the polar night jet was undergoing major distortion prior to breaking down completely a few days later. At the earth's surface, the general fall of pressure experienced over southern England was also felt over a vast area stretching from 65N to 45N, and 20W to 20E, during the 36 hour period up to 00 UTC on the 26th.

Figure 3. Sketch map showing the position of radiosonde stations used in the case histories in this paper. LK = Long Kesh (03920), AU = Aughton (03322), HE = Hemsby (03496), VA = Valentia (03953), CA = Camborne (03808), CR = Crawley (03774), and C7L = Atlantic ocean station occupied by UK Ocean Weather Ship Cumulus, callsign GACA.

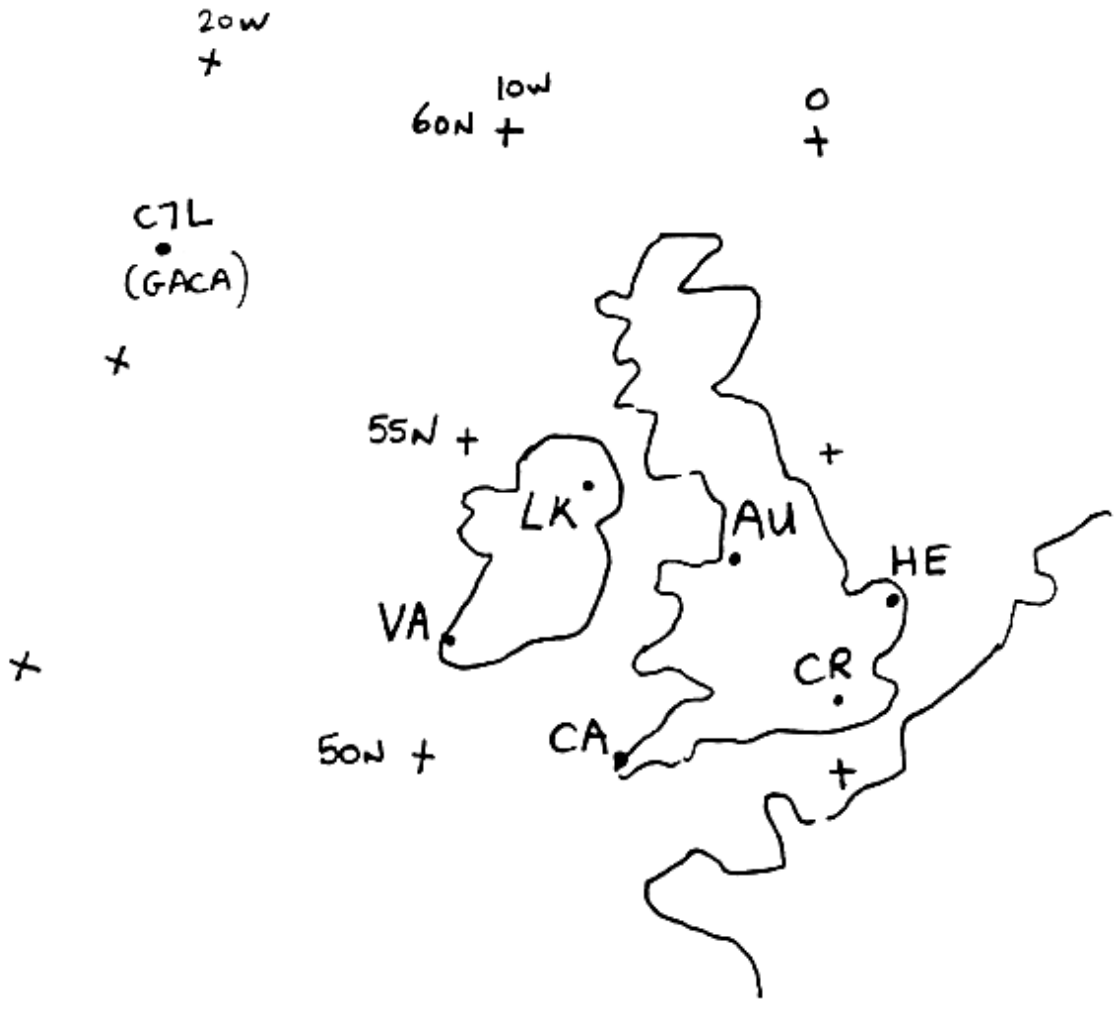

Fig 3.

Case 2. A maturing depression crossing the British Isles on 28 October 1989.

This depression translated from southern Ireland into the central North Sea, and was responsible for a damaging gale in southwest England. Radiosonde ascents at 12 hourly intervals, for Aughton (03322), Hemsby (03496), Crawley (03774, Camborne (03808), Long Kesh (03920) , and Valentia (03953), (see Fig 3 for locations of these stations), are analysed for the period 0000 UTC on 27 October 1989 to 1200 UTC on 29 October 1989, and factors influencing the track and depth of the surface low identified. This case appears typical of many of those studied in the past 5 years, and has many features which may be universal in mid-latitude depressions at this stage of development. The ascents are examined in two ways, firstly by the thickness budget method, and secondly using isentropic analysis, enabling the behaviour of the lower stratosphere to be explored in greater detail, to illustrate the scale of vertical motion present there.

Figure 4a reveals the signature left by the passage of the 100 to 300 hPa thermal anomaly across Aughton, together with the tropospheric thickness warm/cold couplet, and the resulting 1000 hPa geopotential changes. The centre of the surface low passed very close to the station near 1800 UTC on the 29th. Trends in thickness and 1000 hPa height change before and after this time have been extrapolated to show the probable values as the surface low crossed. Note that the 100 hPa geopotential changes by only 3 gpdam over the whole period up to and including the passage of the surface low, and that in this case the 100 hPa may be considered to be the undisturbed level, or lid level referred to by HF. Thus, in this case, almost all the changes that occurred in the 1000 hPa geopotential, and therefore in surface pressure, were the result of thermal changes that which took place between 100 hPa and 1000 hPa. Of these changes, those taking place between 100 and 300 hPa contributed in a positive (thermal) sense, and those in the troposphere in a negative one. Also evident in this case is that near the time of the surface low passage, tropospheric air was at its coldest, and lower stratospheric air at its warmest.

In Figure 4b, the passage of the lower stratospheric warm anomaly is picked out as it crossed Camborne, and 12 hours later, as it crossed Hemsby, stations about 550 km apart, and roughly in a line parallel to the direction of motion of the system. Actual thickness values at 12 hour intervals in the 100 to 300 hPa layer are plotted, together with the thermal winds in the same layer. The similarity in respect of the shape of the anomaly, and the direction and strength of the thermal winds is notable, and suggest that at this level the anomaly was in a quasi-steady state over this period. A translation velocity of about 13 m/s is indicated, less than the advection on the forward side of the anomaly, but slightly more than on the rearward side. Advection of the thermal wind on the forward side of the anomaly at Camborne at 28 0000 UTC was 16 m/s, and at Hemsby 12 hours later was also 16 m/s. On the rearward side, advection of the thermal wind at Camborne was 9 m/s,

and at Hemsby 7 m/s. The difference between the translation velocity and the forward and rearward advection rates indicate that the thermal anomaly was being maintained by dynamically induced adiabatic changes linked to vorticity gradients in the flow at that level. On the forward side air in the 100 to 300 hPa layer must have been ascending and cooling to account for the apparent lateness in arrival of the anomaly compared with advection, while on the rearward side, air was descending and warming because the anomaly arrived over Hemsby earlier than the advection rate indicated.

In order to verify the presence of vertical motions associated with the thermal anomaly in the 100 to 300 hPa layer, analysis was performed in isentropic co-ordinates, using data from the previously listed radio-sonde ascents, taking advantage of the equality in equation 7. The pressure at which the 340°K and 380°K potential temperature isopleths were located on the Aughton ascents is shown plotted against time in Figure 5. Two features stand out; 1) the rise in thickness in the 100 to 300 hPa layer between 0000 and 1200 UTC on the 28th October (see Fig 4a) was accompanied by descent of the 340°K potential temperature surface from 172 to 255 hPa. 2) during the same period the 380°K surface fell by a much smaller amount. If it is assumed that the observed temporal changes in the level of the potential temperature surfaces over Aughton is equivalent to an adiabatic change in the layer temperature in the spatial domain, then it would be expected that the lower stratospheric upwind flow is descending and the downwind flow ascending. The difference in levels between the isentropic surfaces is an indication of the vertical stretching and contraction of the layer, equivalent to a measure of changes in vorticity in the layer. Increasing separation would be associated with increasing vorticity and vice-versa, as expected from equation 7. Thus, the period prior to the passage of the thermal anomaly, and the surface low, was marked by increasing relative vorticity, and the period after 0000 UTC on the 29th was one of decreasing relative vorticity.

The picture that emerges from this observation is most interesting. As stated earlier, it is usual to find a level in the stratosphere which is relatively undisturbed during periods of development or change in the atmosphere below. As changes in vorticity in a layer will necessarily cause changes in thickness, via induced adiabatic motion, then the location of the undisturbed layer implies that it is also one at which there is minimal, if any, changes in vorticity along the flow. It should be noted that the converse need not be true, namely that a change in thickness does not imply changing vorticity along the flow. This is because air is not constrained to flow along horizontal surfaces, but can flow along sloping surfaces without experiencing any change in relative vorticity.

However, vorticity is closely linked to the strength of the flow (Eq 4), and it would be expected that the greatest departure of vorticity from some average value would be found near the level of the maximum wind, which implies that vorticity will decrease upwards and downwards from that level, (see Fig 6). Consider, then, a column of air between the surface and the undisturbed

level, as it traverses the entrance region of a vorticity maximum. The column stretches, but by varying amounts, little at the top and bottom, but rather more near the level of the maximum wind. At the very top the air is experiencing no stretching, the air is flowing in a quasi-horizontal fashion with small or no thickness change at this level. Thus air in the column at all levels below this must be descending in response to the increasing vorticity and associated stretching as it approaches the vorticity maximum. The only way in which the sign of vertical motion in this scenario could differ in the upper and lower parts of the column would be for vorticity centres of opposite sign to overlay each other. This could happen, for example, if a pressure trough, often a region of vorticity maximum, tilted with height, due to baroclinicity, and the centres of vorticity maximum would not be vertically aligned within the column.

A schematic conceptual model of the path of the airflow flowing through a region of changing vorticity is shown in Figure 6. This is obviously a highly simplified model of what can be a very complicated structure in the real atmosphere, but one that will illuminate the main points of the concept. The numbers in the rectangles represent a measure of the vorticity, and are for illustrative purposes only. The changes in shape of the rectangles represents the stretching and contraction of the column. The important point to appreciate is that the region between the undisturbed layer and the level of the maximum wind, usually the lower stratosphere, is a dynamically active region

Figure 4a. Case 2, radiosonde data for Aughton, period 27th to 29th October 1989. From top to bottom, 100 hPa geopotential, 100 to 300 hPa geopotential thickness, 300 to 1000 hPa geopotential thickness, 1000 hPa geopotential. Units are departure from the period mean, gpdam. Note that the lower stratospheric thermal wave is in anti-phase with the tropospheric thermal wave, and that the trough at 1000 hPa is in large part due to the warm anomaly in the 100 to 300 hPa layer. Extrapolated trends in the period 28th 1200 to 29th 0000 UTC are shown dashed.

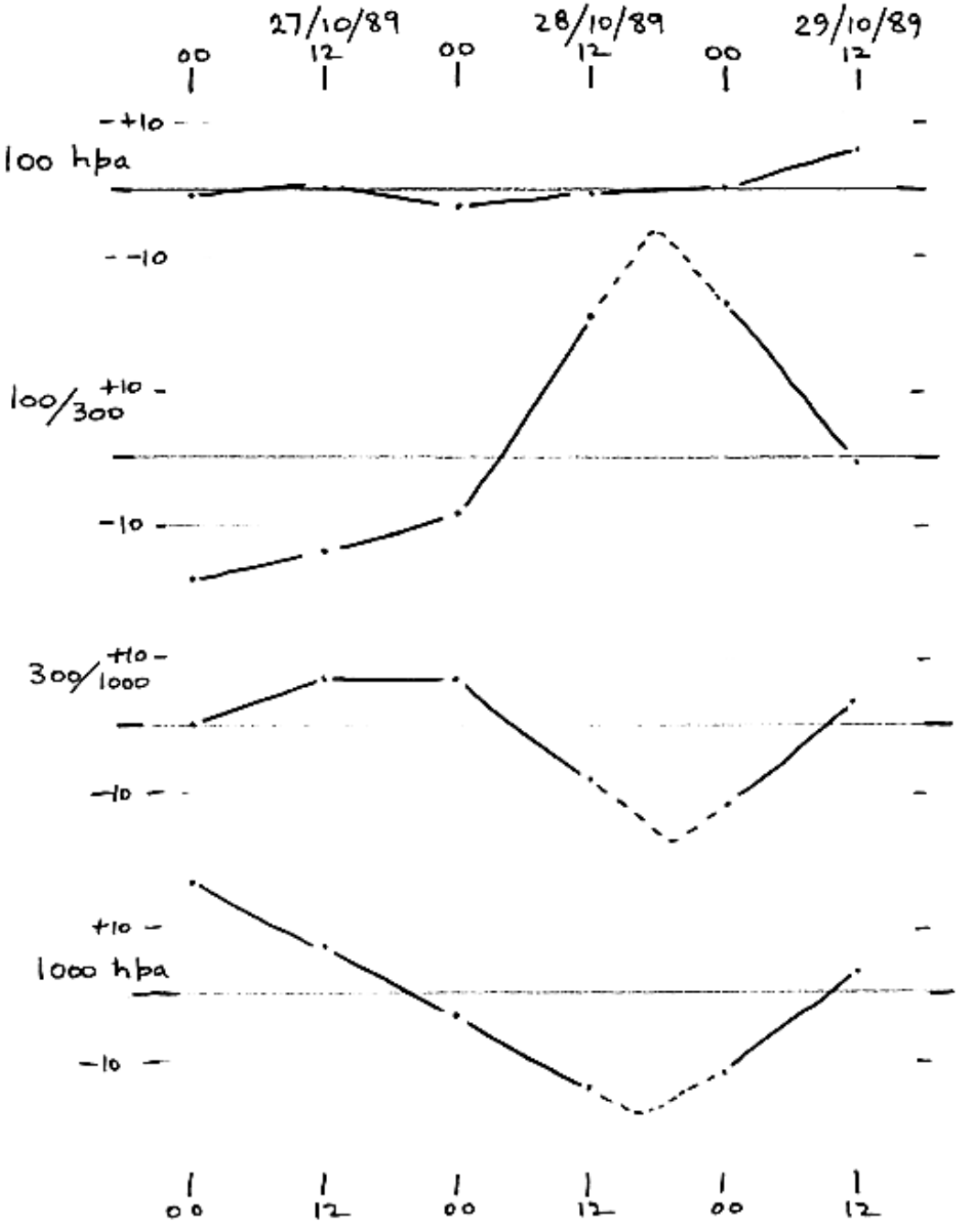

Fig 4a

Figure 4b. Case 2. Lower stratospheric, 100 to 300 hPa, thickness plots for Camborne (solid) and Hemsby (dashed) over the period 27th to 30th October 1989, showing the passage of a thermal anomaly at these two stations located about 550 km apart. Also shown are thermal wind arrows in the 100 to 300 hPa layer at Camborne and Hemsby, illustrating their similarity, and indicating that the warm anomaly was in a quasi-steady state as it crossed the UK.

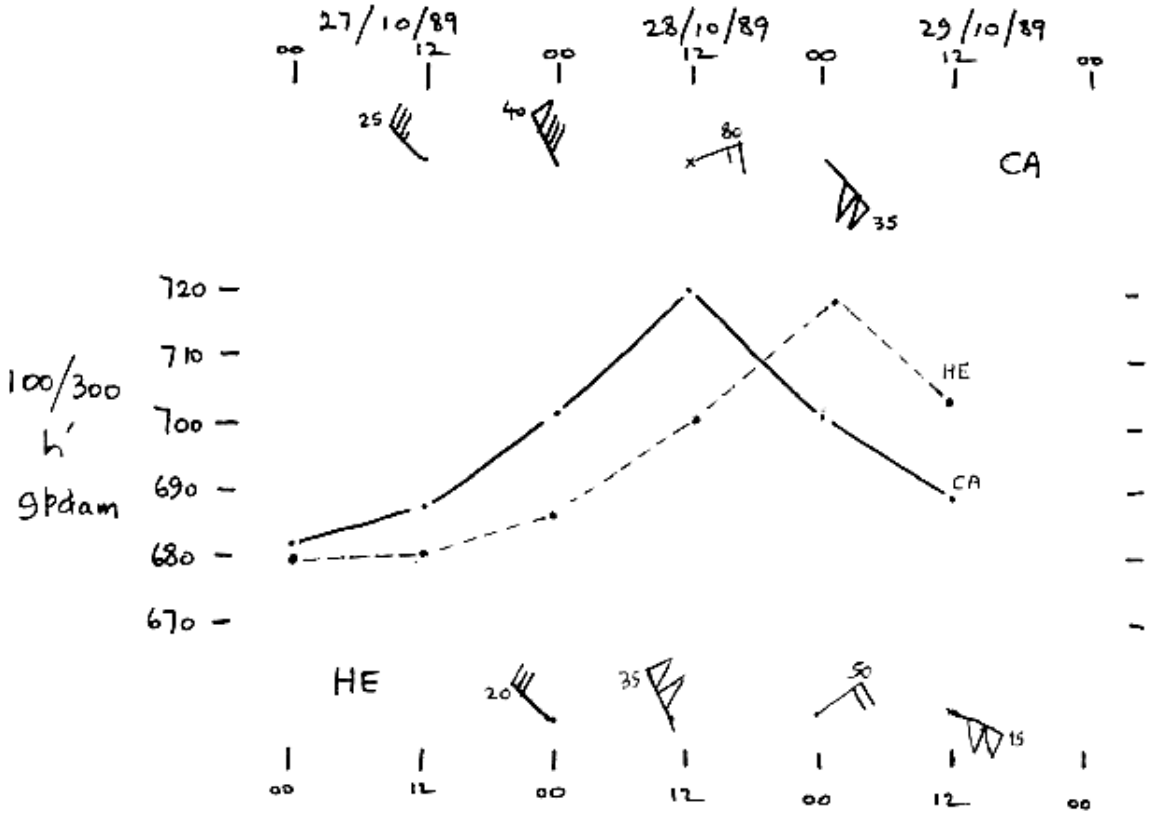

Fig 4b

Returning to case 2, Figure 7 shows a combined spatial and temporal isentropic analysis on the 340°K surface. To achieve this, data for the period 0000 UTC on the 28th to 0000 UTC on the 29th , for the southern United Kingdom radiosonde stations, has been combined and plotted, with the assumption that the entire system moved at a constant rate, and was in a steady state for the 24 hour period. The movement vector used was 230 degrees, 13 m/s, derived from timing the thermal anomaly in the 100 to 300 hPa layer across the domain. Winds, in knots, are plotted relative to the system. Isopleths are in hPa. There is evidently ascending motion on the easternmost plots. Interestingly, ascending motion is also found to the south-west of the centre, but over the region generally wind directions are closely aligned with the isentropes. The degree of uncertainty as to the exact shape of the isentropes, a result of the temporal and spatial disposition of the data, precludes a quantitative analysis of vertical motion. It is possible that air was descending close to, and just to the east of the centre, and also on the extreme western edge, but no well defined region of descent is evident. This negative result would indicate that the developmental stage of the system may have already ended. In this respect the surface pressure was at its lowest near 1200 UTC on the 28th, and it could be that the maturation of this system was accompanied by a cessation of descent in this layer, this being replaced by neutral or slightly ascending motion. This implies that the warm anomaly would subsequently slowly erode, and allow the associated tropospheric trough to relax.

Figure 5. Case 2. Pressure at which the 340°K and 380°K potential temperatures were found over Aughton between the 27th and 29th October 1989, prior to and during the passage of the lower stratospheric thermal anomaly shown in Fig4a. The difference in pressure between the two isentropic surfaces is a measure of the stretching and contraction of an air column between the isentropes.

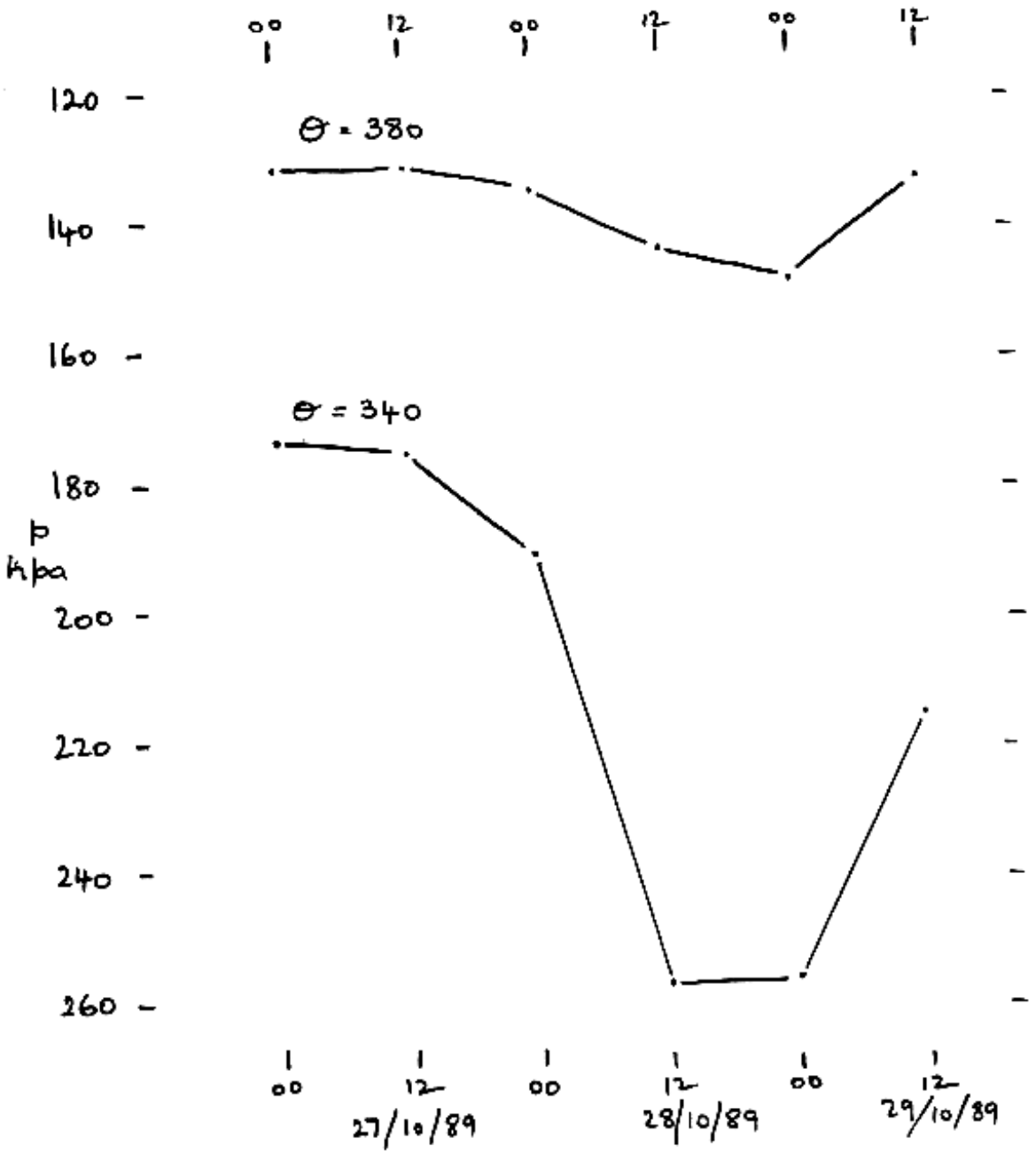

Fig 5.

Figure 6. Simplified conceptional model of the vertical excursions experienced by an airflow moving through patterns of vorticity. The shape of blocks represents the stretching and compression which accompany changes in vorticity. The numbers in the boxes represent the vertical separation in pressure co-ordinates of fixed isentropic surfaces.

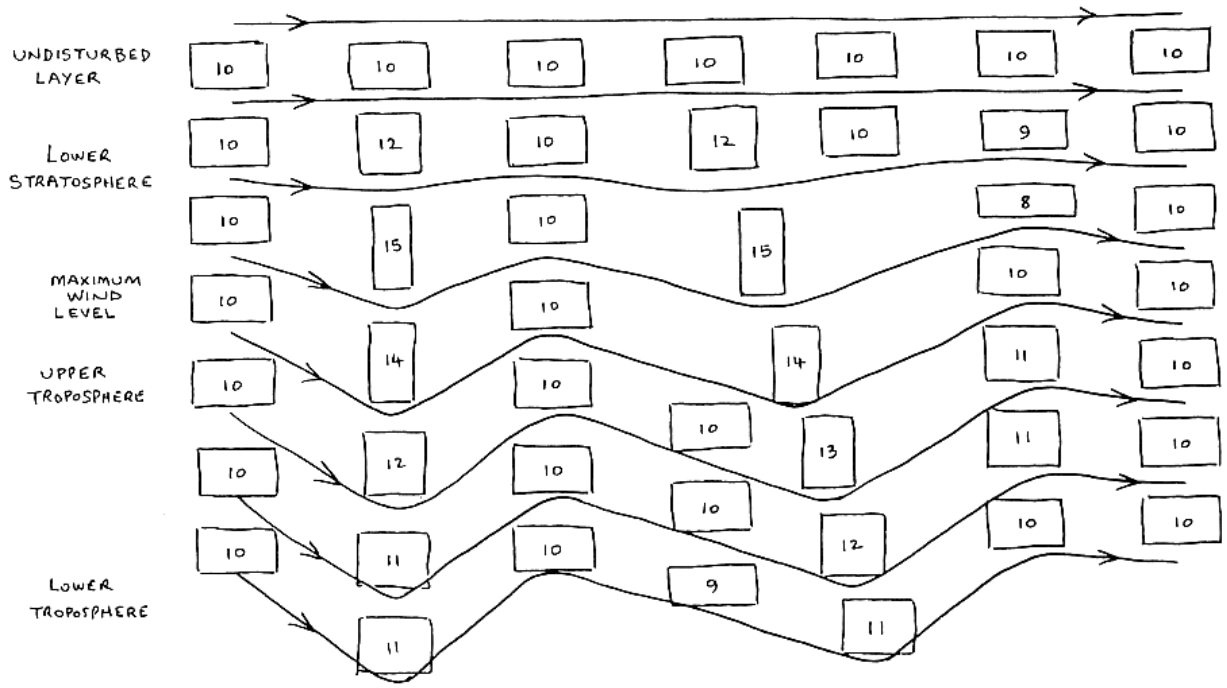

Fig 6

Figure 7. Case 2. Extended isentropic analysis, on the 340°K surface, as at 1200 UTC on the 28th October 1989. Isopleths of pressure, (solid) are drawn at 10 hPa intervals. Winds are shown with convectional arrows, speed in knots. The extended analysis assumes that the whole system is in a quasi-steady state for 48 hours as it moves across the domain.

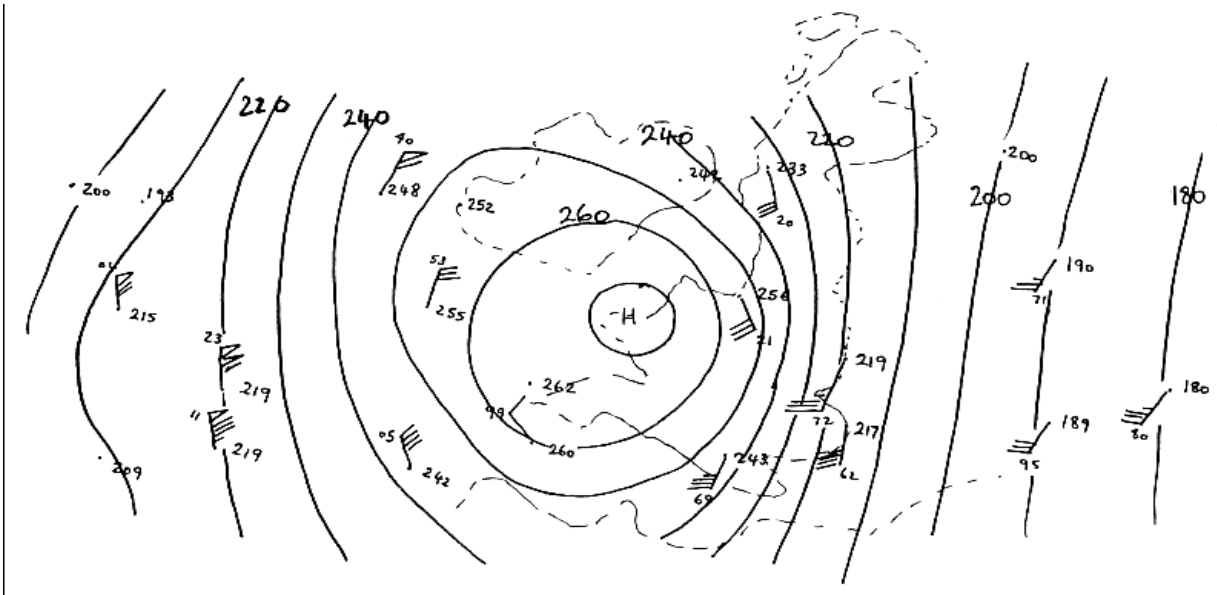

Fig 7

Figure 8. Case 3. Path taken by deepening surface low over the eastern North Atlantic ocean, 13th to 15th October 1990. position and pressure of the low centre shown at 6 hour intervals. The position of ocean station C7L is also shown.

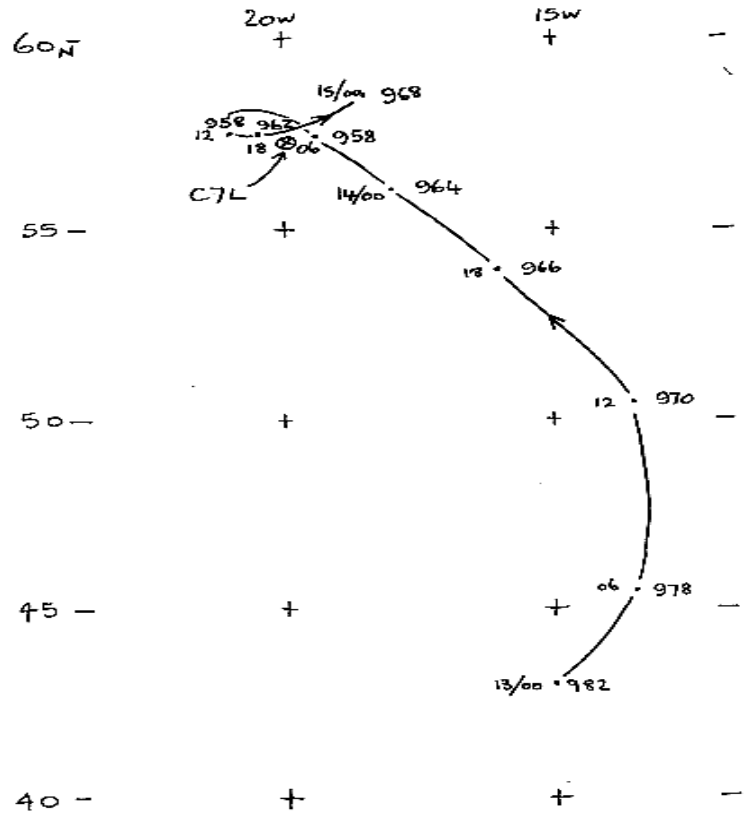

Fig 8

Case 3. A depression moving northwards and deepening over the eastern North Atlantic ocean, 13th to 15th October 1990.

This depression was studied using the 6 hourly routine radio-sonde ascents released from the UK Ocean Weather Ship Cumulus, call sign GACA, located near 57 N 20 W, a position that used to be known as station Lima (C7L). The track of the depression is shown in Figure 8, while it deepened from 982 hPa to 958 hPa, passing conveniently close to the weather ship at the time of lowest pressure. Geopotential and thickness data at GACA for the entire period is tabulated in Table 5a, while the thickness budget is shown in Table 5b. It is gratifying, and a tribute to the onboard meteorologists, that data was available up to 20 hPa on each of the 9 soundings during the period of this study, providing a complete picture of the sequence of events unfolding above the ship.

Table 5a. 20 and 1000 hPa geopotential and partial thickness for selected layers between 20 and 1000 hPa over GACA, 13th to 15th October 1990. Units gpdam.

	13/00	13/06	13/12	13/18	14/00	14/06	14/12	14/18	15/00
20 hPa	2636	2635	2636	2637	2644	2643	2643	2641	2642
20 to 30	258	259	258	261	261	259	263	261	261
30 to 100	773	771	771	768	774	776	774	776	775
100 to 300	716	711	708	711	719	730	732	726	723
300 to 1000	891	896	903	912	915	911	906	907	903
1000 hPa	-2	-2	-4	-15	-25	-33	-32	-29	-20
MSLP	998	997	995	982	970	961	963	965	976

Table 5b. Thickness budget, 6 hour partial thickness changes and resulting change in 1000 hPa geopotential, ending at the time shown. Units are gpdam.

Layer hPa	13/06	13/12	13/18	14/00	14/06	14/12	14/18	15/00
Above 30	+2	-2	+2	-7	-1	+4	0	-1
30 to 100	-2	0	-3	+6	+2	-2	+2	-1
100 to 300	-5	-3	+3	+8	+11	+2	-6	-3
300 to 1000	+5	+7	+9	+3	-4	-5	+1	-4
Total	0	+2	+11	+10	+8	-1	-3	-9
1000 hPa	0	-2	-11	-10	-8	+1	+3	+9

It is clear from Tables 5a and 5b that the surface pressure and 1000 hPa geopotential commenced a long period of falling tendency near 0000 UTC on the 13th , culminating, at or near 0600 UTC on the 14th, with a surface pressure near 960 hPa, after which time a slow rise was observed. As can be seen from Fig 8, it was at about that time that the surface low was at its

deepest, and coincidentally was located near its closest approach to GACA, at a distance of some 50 km. During the period of falling pressure, Tables 5a and 5b show that for much of the time there was tropospheric warm advection over GACA, with the 300 hPa to 1000 hPa thickness rising from 891 gpdam at 0000 UTC on the 13th, to 915 gpdam 24 hours later, thereafter dropping unsteadily away to 903 gpdam at 0000 UTC on the 15th. The peak tropospheric thickness value occurred, however, at least 6 hours before the lowest surface pressure at GACA. In fact, as Table 5b shows, the peak increase in tropospheric thickness occurred between 1200 and 1800 UTC on the 13th, and although this was the period of the greatest fall in 1000 hPa geopotential, it was the increasing thickness values in the lower stratosphere between 1200 UTC on the 13th and 0600 UTC on the 14th which took over as the main agent responsible for the continuing fall in surface pressure.

After 0600 UTC on the 14th, surface pressure started to rise, in response to continued tropospheric cooling, and an initial reduction in lower stratospheric warming, which changed to marked cooling after 1200 UTC on the 14th. The coincidence for the timing of the lowest surface pressure, and the peak in lower stratospheric thickness, by extrapolation, near 0900 UTC on the 14th, should be noted.

The principle of the thickness budget approach, its simplicity and ability to highlight the importance in lower stratospheric thickness is illustrated in Figure 9, where the time series of geopotential for 100, 300 and 1000 hPa are plotted, together with the 100 to 300 hPa and 300 to 1000 hPa thickness values. The slight geopotential ridge at 100 hPa, which reached a peak value near 0000 UTC on the 14th, seems to have been related to an event much higher in the atmosphere, as can be seen from Table 5a, where the 20 hPa geopotential is seen to experience an interesting step-like rise of 7 gpdam, indicating the passage above this level of a front-like decrease in net thickness. Also of interest in this respect, in the 20 to 100 hPa layer, is the almost total compensation to the step change, where thickness values increased by 6 gpdam during the same period. The vertical cooling.warming couplet is suggestive of a dynamic forcing mechanism at work, and this is looked at again in a later paragraph.

The correspondence between the lower stratospheric thermal field and the geopotential field in the upper troposphere is one of the most important links associated with tropospheric and surface development. The examples shown here are not unique but rather commonplace. The importance of this link cannot be stressed too much. The changes in direction and strength of the upper tropospheric flow, which is largely instrumental in creating the conditions necessary for much of the weather we experience, depend fundamentally on the geopotential field at some much higher level in the atmosphere, and changes in the intervening thermal field. The upper tropospheric geopotential field can only change if either or both of those change.

Thermal changes over a point can be considered as being composed of three components, 1) advective change, 2) thermal change due to adiabatic adjustment, 3) diabatic thermal changes. When considering the lower stratosphere, the third component would normal be very small compared the the other two, or absent, and on small time scales can be ignored.

If Vn is the wind vector normal to the thermal gradient, and Φ is the difference between the local and adiabatic lapse rates, and where ω is the vertical velocity in pressure co-ordinates, then the local rate of change of thickness h', in a layer bounded by fixed pressure levels p_u and p_l is given by:

$$\partial h'/\partial t = Vn*dh'/ds + R/g \left[\int^{pu}_{pl} (\Phi * \omega)\right] d(\ln p) \qquad 10.$$

The first term on the right hand side being the advection of thickness by the local wind, and the second term the change in thickness due to vertical motion.

Turning back to the example, case 3, and the serial soundings at weather ship GACA, rather more information concerning the behaviour of the lower stratosphere can be obtained by careful analysis of the thermal winds calculated from the soundings and their implied thermal gradients. From a knowledge of the geostrophic wind at any two levels in the atmosphere, the thermal wind vector can be calculated, and from this the local thickness gradient obtained. Combining this with the geostrophic wind vector normal to the thickness gradient, the local rate of thermal advection can be found. Taking the mean of values from the start and end of a 6 hour period as being equal to the true mean for that period, then the total thermal advection in a layer over a 6 hour period can be compared with the actual change in thickness observed, with the non advective component appearing as the difference between the two. This component will be largely determined by adiabatic changes brought about by vertical motion. Bearing in mind the stably stratified nature of the temperature lapse in this lower stratospheric 100 to 300 hPa layer, then even modest vertical motion in only part of the layer will produce a detectable change in thickness.

Figure 9. Case 3. Plots of geopotential and thickness over C7L, 13th to 15th October 1990. Units are gpdam relative to the period mean. The upper graph is for the 100 hPa geopotential. The central graph shows the 300 hPa geopotential (solid) and the 100 to 300 hPa thickness (dashed). Lower graph shows the 1000 hPa geopotential (solid) and the 300 to 1000 hPa thickness (dashed).

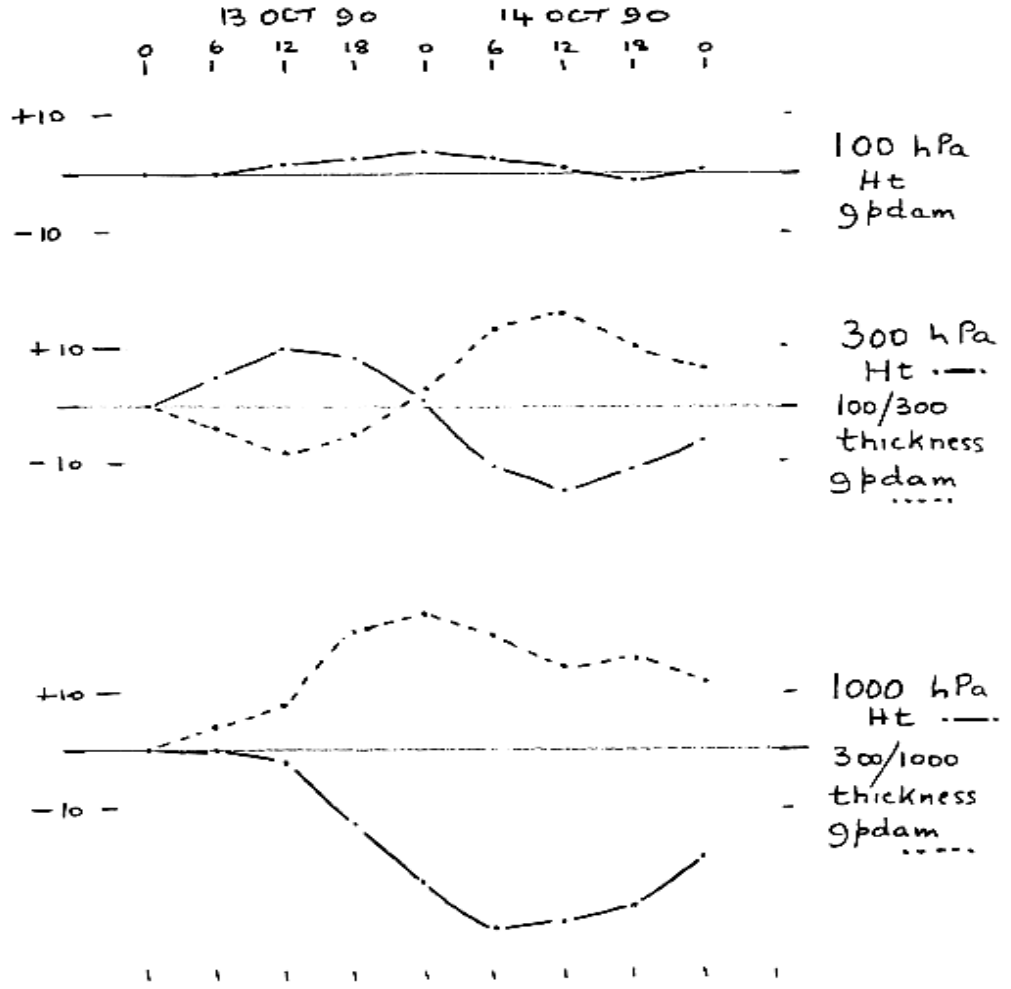

Fig 9

Figure 10a. Case 3. Advective (solid) and non-advective (dashed), thickness changes in the 100 to 300 hPa layer over C7L, 13th and 14th October 1990. Changes are over 6 hour intervals, plotted against time of ending. Units are gpdam. For non-advective changes, positive values indicate descent (D), and negative values ascent (A).

Figure 10b. Upper graph, as Fig 10a, but for the 30 to 100 hPa layer. Lower graph is the 1000 hPa geopotential.

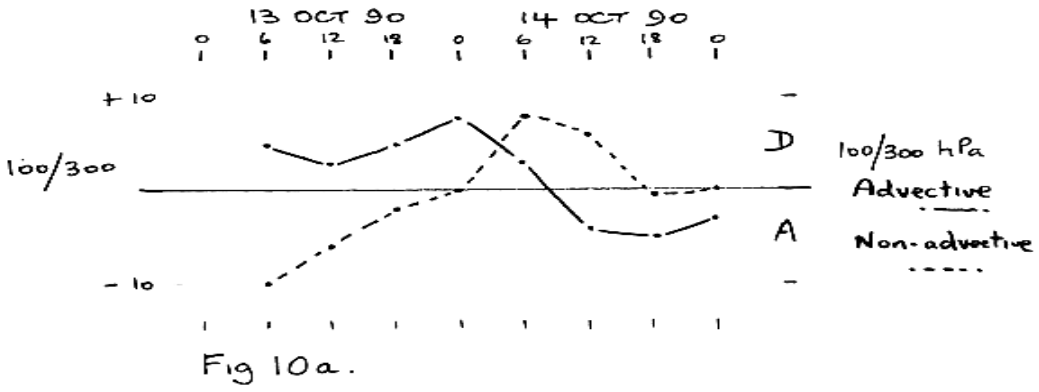

Fig 10a.

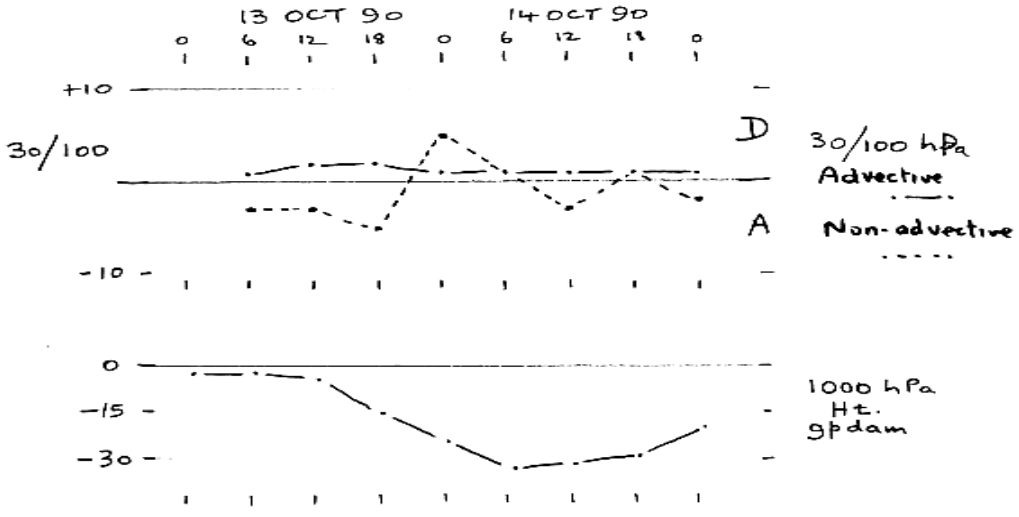

Fig 10b

In making the the calculation of thermal wind in the 100 to 300 hPa layer in this case, it is recognised that ageostrophic components could be present in the observed winds, especially at 300 hPa where there was considerable curvature in the contours. As the correct application of the thermal wind equation requires geostrophic balance, relevant upper air charts for the main synoptic hours were examined, and an estimate made of the curvature of the contours in the vicinity of GACA was made. The local speed change and vertical shear were also examined, but the data was too sparse and the uncertainties in these values too large for any reliable adjustment to be made for these factors. However, the observed winds at 300 hPa were adjusted to give geostrophic values after allowing for curvature. No adjustment was deemed necessary at 100 hPa where the flow was much lighter.

The calculated 6 hour thickness changes divided into advective and non advective, (dynamic), are shown in Figure 10a for the 100 to 300 hPa layer, and in Figure 10b for the 30 to 100 hPa region of the stratosphere. In Figure 10a it can be seen that as the deepening surface low approached GACA , the lower stratosphere over GACA experienced continuous warm advection, amounting to an average of approximately 0.8 gpdam per hour. However, before 0000 UTC on the 14th, dynamic changes in that layer were leading to cooling (ascent), which up to 1200 UTC on the 13th was sufficient to entirely offset the warm advection and actually resulted in a net cooling in the layer over ship GACA. The dynamic cooling decreased steadily until 0000 UTC on the 14th, by which time it was close to zero, and the continuing warm advection led to the surge in thickness in this layer over GACA seen in Figure 9. By 0600 UTC on the 14th, quite a dramatic change occurred, for although warm advection was still in evidence, dynamic descent had replaced ascent, and was of sufficient intensity to lead to more than 1 gpdam per hour thickness increase, a rate that was maintained until after 1200 UTC on the 14th. However, already by that time the intense dynamic warming was being offset by cold advection which continued until the end of the period. Also, the dynamic descent was replaced by a near neutral flow, and the 100 to 300 hPa thickness fell due to the cold advection alone.

The picture that emerges is pretty much identical to that found in case 2 by using isentropic analysis to pinpoint the areas of dynamic ascent/descent in the vicinity of a lower stratospheric thermal anomaly. As in case 2, the flow in the region downwind of the thermal anomaly in the 100 to 300 hPa layer was found to be ascending while upwind of the anomaly it was descending.

The graph of 6 hour thickness change in the 30 to 100 hPa layer, Figure 10b, is interesting as it shows that this layer was also dynamically active in this case. There was an almost constant rate of warm advection of about 0.15 gpdam per hour, but this was at times dwarfed by fairly large swings between ascent and descent. The step change between 1800 UTC on the 13th and 0000 UTC

on the 14th looks significant, when ascent sufficient to produce cooling of nearly 1 gpdam per hour was replaced by descent of almost equal magnitude. The arrival of this pulse of peak descent in the 30 to 100 hPa layer, occurring 6 hours before a peak of the same sign in the 100 to 300 hPa layer, may be speculatively linked to wave action in the lower stratosphere.

It should be pointed out here that no account has been taken of the possible radiative affects, which would be expected to produce a net cooling in the lower stratosphere at this time of the year, over the two day period under consideration.

The importance of the features revealed by this analysis are worth repeating. There is evidently a balance and interplay between dynamic and advective changes occurring in the stratosphere, which are most pronounced at lower layers, and which are important because of the influence they have on the development and decay of upper tropospheric features, which are controlled by the, sometimes subtle, changes in the overlying thermal pattern.

Case 4. A deepening Atlantic low, 26th to 29th January 1989.

During the three days starting the 26th January 1989, a strong zonal flow existed over the Atlantic at mid-latitudes, and a tropospheric baroclinic wave amplified as it moved from a position near 42 N 42 W on the 25th, to 63 N 18W on the 27th. The resulting surface low deepened from 998 to 958 hPa in the same period. The deepening disturbance passed close to the UK weather ship GACA, then located on station C7L, near 57 N 20 W., and the routine 6 hourly radiosonde ascents from that ship are used to examine the behaviour of the atmosphere above during that period.

Data was available up to 100 hPa on all 12 ascents over the 3 day period, with 8 reaching 30 hPa, and three 10 hPa. The geopotential at 10 hPa was falling markedly over the period, with a drop of 59 gpdam recorded between the 26th and 29th. Winds at 10 hPa were of jet strength throughout, 65 m/s being typical. At 30 hPa a more modest fall in geopotential of 34 gpdam was recorded over the same period, indicating a net cooling of 25 gpdam in the 10 to 30 hPa layer. As the thermal wind direction in the layer was near 300 degrees for most of the 3 day period, and the 30 hPa wind direction was about 250 degrees, indicating warm advection, there was obviously a very strong non-advective component to the change in the 10 to 30 hPa layer, and with the sign of the change being negative, indicating ascent. Lower down, at 100 hPa, the net geopotential change was only 6 gpdam in the same period, showing that, just as with the 10 to 30 hPa layer, cooling had taken place in the 30 to 100 hPa layer, to the extent of 28 gpdam, giving a total cooling of 53 gpdam in the 10 to 100 hPa layer, equivalent to a decrease in mean temperature of nearly 8°K.

Turning to the lower stratosphere, and the 100 to 300 hPa layer, there is once again a general cooling trend evident, but with a warm anomaly embedded in the flow, and which passed GACA

between 1200 UTC and 1800 UTC on the 27th. Figure 11a shows this clearly. Included in this figure are time series plots of 100, 300 and 1000 hPa geopotential, and thickness for the 100 to 300 hPa layer, and the 300 to 1000 hPa layer. Also plotted are wind arrows for the 100 and 300 hPa levels, and for the thermal wind in the 100 to 300 hPa layer, and the 500 to 1000 hPa layer, this latter being included to give a feel for the movement and development of the tropospheric baroclinic wave.

From Figure 11a, it can be seen that the deepening low was nearly in phase with the tropospheric baroclinic wave, with a preliminary minimum in surface pressure/1000 hPa geopotential at 1800 UTC on the 26th, which resulted as the peak tropospheric thickness values crossed the location. However, the driving feature, a trough in the upper tropospheric jet stream, can be seen from the 300 hPa wind arrows to have crossed GACA nearly 24 hours later. Also it can be seen from Figure 11a that the evolution of the 300 hPa wind field over GACA was tied to the passage of of the lower stratospheric warm anomaly, and its associated thermal wind field. Several of the features shown schematically in Figures 1a and 1b can be identified in the wind arrows shown in Figure 11a. This warm anomaly, in the presence of a fairly steady south-westerly flow of about 50 m/s at 100 hPa, led to the observed increase in the 300 hPa wind from 45 m/s at 1800 UTC on the 26th , to 75 m/s at 0600 UTC on the 27th. As the lower stratospheric warm anomaly passed by, the thermal wind in the 100 to 300 hPa layer rotated counter clockwise, and the 300 hPa wind veered in response, marking the passage of the geopotential trough at that level.

Interestingly, in this example, the lower stratospheric and tropospheric thermal waves are almost in anti phase, so that the fall in 1000 hPa geopotential was limited, with a relatively cold lower stratosphere over a warm troposphere, and vice-versa later. However, a secondary minimum on 1000 hPa geopotential, which occurred near 0600 UTC on the 27th, was clearly the result of changes taking place above 100 hPa. For instance, during the two 6 hour periods between successive surface pressure minima, the changes in the 100 to 300 hPa thickness were +1 and +8 gpdam, compared with changes in tropospheric thickness over the same period of –2 and –8 gpdam. As these thermal changes almost cancel, the observed changes of +2 and –6 gpdam in the 1000 hPa geopotential must be virtually the same as the changes in 100 hPa geopotential, which at +1 and -6 gpdam, they clearly are, and which in turn owe their origins to changes in total thickness in the atmosphere above 100 hPa.

As in case 3, using 6 hourly serial ascents, a detailed analysis of the rate of advection compared with the observed changes in thickness in the 100 to 300 hPa layer was undertaken. Unlike that case, adjustments to the observed winds to account for ageostrophic effects have not been made in case 4. Figure 11b shows the 6 hour thickness change in the lower stratosphere, divided into its advective and dynamic components. Where this latter is negative, mass ascent in the

layer is indicated, and where positive, descent. These are shown as A and D in Figure 11b. Significant features in this case are the continuous and increasing ascent indicated up to 1200 UTC on the 27th, with a slight decrease between 1200 UTC and 1800 UTC on the 27th, then a dramatic change to descent by 0000 UTC on the 28th, with sustained and fairly intense descent continuing throughout that day. Figure 11b should be considered in conjunction with the plotted wind arrows for 300 hPa in Figure 11a, where it is evident that the increasing ascent in the lower stratosphere was associated with strengthening flow ahead of the 300 hPa trough. The switch to descent occurred coincidentally with the passage of the trough, with descent in the strong flow upwind of the trough. This is in agreement with the conceptional model of vorticity change shown if Figure 6.

A rough check for gross errors that may have arisen due to making no allowance for possible ageostrophic effects, chiefly in the 300 hPa winds, the same calculation was carried out for the 300 to 500 hPa layer during the period when this layer was wholly in the troposphere (tropopause at or above 300 hPa), where some non advective effects might be expected from both latent heat release and dynamics, but where both effects are small because of low temperatures and steep lapse rates. After 1200 UTC on the 27th it is likely that the tropopause descended into this layer, in which case some increase in non advective changes might be expected, due to decreasing temperature lapse and vertical motion. During the period 0000 UTC to 1800 UTC on the 26th, the calculated advective changes in the 300 to 500 hPa layer was +15 gpdam, compared with an actual change of +13 gpdam. In the following 12 hours up to 0600 UTC on the 27th, the calculated and observed changes were –2 and –3 gpdam respectively. These results suggest that the 300 hPa wind was relatively uncontaminated by ageostrophic effects, and that no gross error is likely in the 100 to 300 hPa advective and dynamic changes shown in Figure 11b.

A further point to note from the calculation plotted in Figure 11b is that, for most of the period, the sign of advective change was opposite to the sign on non-advective change. This highlights the fine balance that exists at this lower stratospheric level, between advective and dynamic effects. Enhancement or decay of thermal anomalies may be envisioned due to feedback between the two. It seems probable that marked development can occur, in the first instance at upper tropospheric levels, but eventually affecting all levels down to the surface, when either the countering effect of ascent/descent on a pre-existing thermal advection pattern changes, perhaps in response to upwind developments. It is certainly evident from these and other (undocumented) cases studied that a situation quite near balance is often observed, with slow but fairly steady changes in the 100 to 300 hPa thickness. But it is thought that there will be instances where feedback can lead to sudden and rapid change in thickness in this layer, as either the advective or dynamic term becomes dominant.

In this case, Figure 11b shows that dynamic ascent changed to descent over ship GACA just before 0000 UTC on the 28th, warm advection had already changed to cold, with the magnitude of the advective term always outweighing that of the dynamic term. This may be compared with Figure 10a where dynamic descent and warm advection were acting in tandem for a time. In the present case the relative weakness of the dynamically induced thickness changes may lead to the possible conclusion that further development of the surface low would be limited. However, this low went on to deepen to have a central pressure of less than 950 hPa near Spitsbergen on the 28th.

So what led to the continued deepening of this depression? It is probable that this is another example of a surface low forced to deepen due to the advection of its associated pulse of warm tropospheric air across a thickness gradient towards warmer values, in this case in the stratosphere or mesosphere. In a semi-Lagrangian frame moving with the tropospheric thermal wave, thickness budget calculations would show steadily increasing thickness values at levels above 100 hPa, The evidence for this if in the GACA data, where, as was noted earlier, there was a south-west to west jet stream above 100 hPa, with wind speeds increasing with height, at least up to the 10 hPa level.

Figure 11a and 11b. Case 4. a) Top to bottom. 100 hPa wind feathers; 100 hPa geopotential: 100 to 300 hPa thermal wind feathers: 100 to 300 hPa thickness (h'): 300 hPa wind feathers; 300 to 100 hPa thickness; 500 to 1000 hPa thermal wind feathers; 1000 hPa geopotential. Plots for station C7L, 26th to 29th January 1989. Standard plotting convection for winds (speed in knots), interpolated missing data shown dashed, height/thickness units are gpdam. b) As figure 10a but for the 100 to 300 hPa layer over the period 26th to 29th January 1989 over C7L.

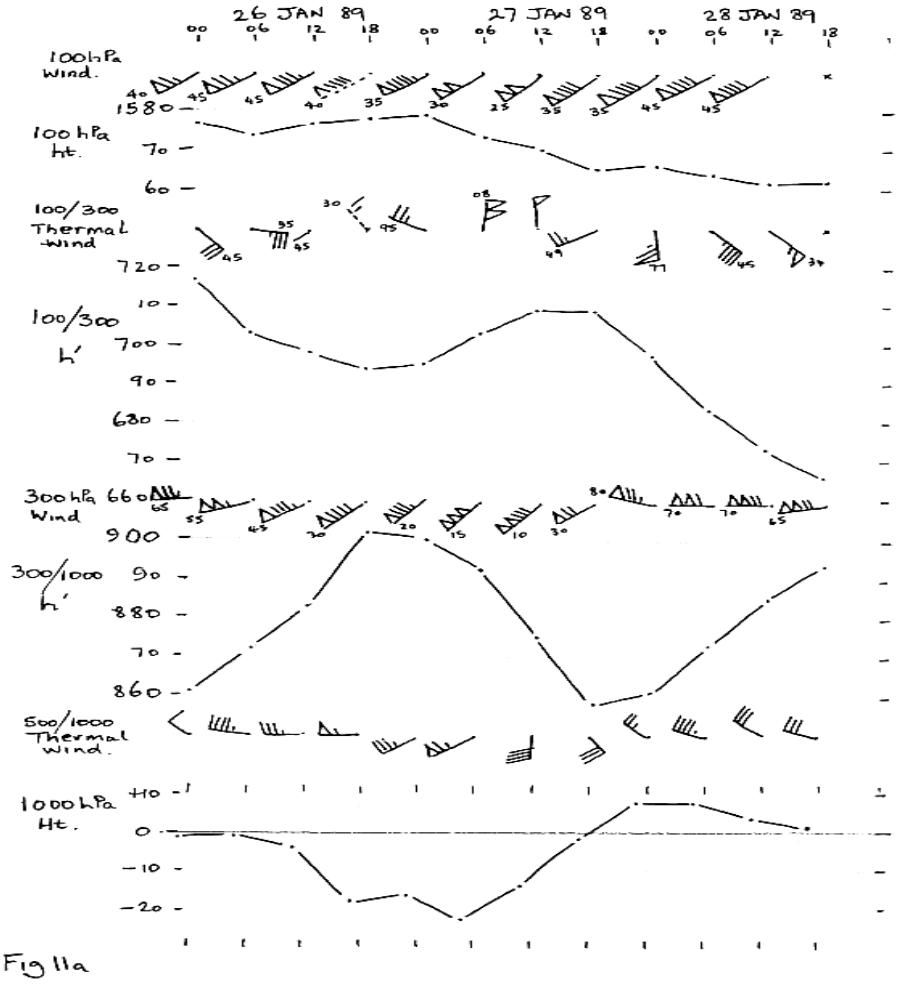

Taking the observed 100 hPa flow at GACA to be representative of that over the region 56 N to 63 N, traversed by the surface low as it deepened from 980 to 956 hPa, then the 47 m/s gradient implies a geopotential gradient of 51 gpm per degree latitude. The fall in surface pressure of 24 hPa is equivalent to a fall of approximately 206 gpm in 1000 hPa height. However, the change in 100 hPa geopotential over the surface low would have been about 350 gpm in the same period, leading the the conclusion that there must have been a net cooling of about 140 gpm between 100 hPa and 1000 hPa over the low centre. It also suggests that there was little contribution to the depth of the surface low from the warm thermal anomaly in the 100 to 300 hPa layer, in agreement with the lack of development implied from Figure 11b. The main contribution by the warm thermal anomaly in the 100 to 300 hPa layer in this case, was to act as a forcing agent aloft, controlling and shaping the upper tropospheric flow, and steering the tropospheric thermal wave on a path that took it towards lower values of geopotential in the stratosphere.

Case 5. Passage of a short-wave trough aloft over Atlantic weather station C7L, 11th to 13th October 1989.

During the two day period in October 1989, ending at 1800 UTC on the 13th, a strong zonal flow covered the north Atlantic at mid-latitudes. Embedded in this flow aloft a short-wave trough with an associated surface ridge/trough couplet, passed close to C7L near 1200 UTC on the 12th and 0600 UTC on the 13th respectively. The trough contained a surface low which deepened from 1000 hPa to 978 hPa while translating from 51 N 40 W to 61 N 05 W. The data, consisting of routine 6 hourly radiosonde ascents from C7L, are analysed and presented in the same way as in case 4.

Figure 12a shows the time history of the 100 hPa geopotential, 100 to 300 hPa thickness, 300 to 1000 hPa thickness, and 1000 hPa geopotential. This system contained a strong baroclinic wave signature in the troposphere, as indicated by the 300 to 1000 hPa thickness. A cold/warm couplet in the lower stratospheric 100 to 300 hPa layer is evident in the time series, which is not quite in anti phase with the tropospheric pulse. The mismatch, in this case, has resulted in the observed surface pressure ridge near 1200 UTC on the 12th, whereby the marked decrease in lower stratospheric thickness between 0600 UTC and 1200 UTC on the 12th, was able to offset the modest tropospheric warming during that period. In fact, it is evident that the surface pressure only fell substantially at C7L when both tropospheric and lower stratospheric thickness values were increasing, between 1800 UTC on the 12th and 0000 UTC on the 13th. The lowest surface pressure occurred near 0600 UTC on the 13th, at which time tropospheric thickness values were falling, but at the same time as there was a sharp increase in lower stratospheric thickness. Surface pressure recovered rapidly, initially due to strong tropospheric cooling and a halt to the lower stratospheric

warming, and latterly due to marked cooling in the 100 to 300 hPa layer as modest warming returned to the troposphere.

Once again, as in Figure 11a, note the quasi-steady nature of the 100 hPa wind, plotted in Figure 12a. However, in this case the 100 hPa geopotential is not quite as steady, and is reacting to the passage above of a net cold anomaly, such that the 100 hPa geopotential rose to a peak near 1800 UTC on the 12th, after which a slow decline set in.

The 100 to 300 hPa thermal winds shown in Figure 12a are interesting. Here there is an almost continuous south-easterly thermal wind. But with considerable modulation in strength. The direction indicates that relatively cold air lay to the south-west of C7L, and relatively warm air to the north-east in that layer. The passage of the warm anomaly in this layer was marked only by a temporary backing to north-east and decrease in the thermal wind. This indicates that the core of the thermal anomaly passed to the north of C7L. However, the veer in thermal wind that occurred by 0600 UTC on the 13th would suggest that the warm core passed before that time.

Figure 12a and 12b, Case 5. a) As figure 11a, except for the period 12th and 13th February 1989, and with the 500 to 1000 hPa thermal winds omitted. b) As figure 10a, for the 100 to 300 hPa layer over the period 12th and 13th February 1989, over station C7L.

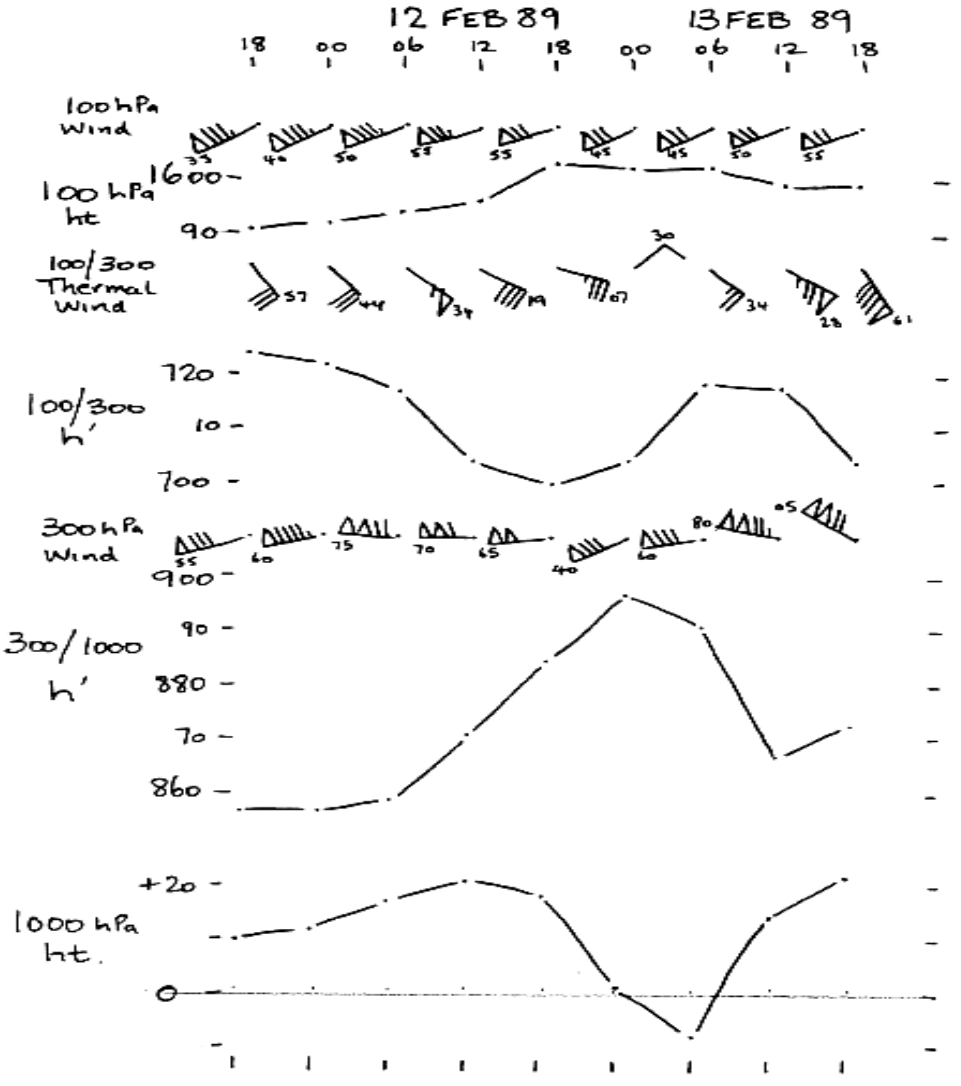

Fig 12a

Although the measured thickness in the 100 to 1300 hPa layer did fall slightly in the 6 hours to 1200 UTC on the 13th, the shape of the plotted thickness in Figure 12a suggests a peak value crossing after 0600 UTC but before 1200 UTC on the 13th. Possible explanations for this are either that the warm core in this layer was complex on the mesoscale, with more than one centre, or that the warm core was intensifying as it crossed C7L. The plots in Figure 12b would suggest that there was some scope for development of the warm anomaly, with dynamic descent stronger than cold advection between 0000 UTC and 1200 UTC on the 13th. The increase in strength of the thermal wind after 0600 UTC on the 13th could also support the possibility of development of the warm anomaly as it moved away from C7L towards the north-east, although the magnitude of the cold advection observed by 1800 UTC on the 13th must also have contributed to the increase in strength of the thermal wind.

Comparing Figure 12b with Figure 11b from case 4, there are a number of striking differences, Firstly, in case 5 there is a total absence of warm advection in the 100 to 300 hPa layer, the passage of the warm anomaly being marked only by a reduction in strength of the cold advection. This continuous cold advection seems to have been associated with an earlier strong warm anomaly which crossed C7L on the 11th, and was still in evidence to the north-east during this period. In case 4, not only was there warm advection for part of the time, but its magnitude was greater than the dynamic warming that took place late in the period. In case 5, there appears to have been continuous dynamic descent throughout, though it was the variation in amplitude of this term which decided if the thickness rose or fell over C7L. It was during the brief period, near 0600 UTC on the 13th, when dynamic warming dominated in the face of strong cold advection, that the warm anomaly was being being maintained, and which in turn was able to modify the lower stratospheric thermal field in such a way as to maintain the 300 hPa trough in the geopotential field, and which was instrumental in driving the tropospheric thermal wave. In this sense, the system can be thought of as being in a positive feedback mode, unlike in case 4, with scope for the warm anomaly in the lower stratosphere to intensify as the system moved away from C7L, and to assist in reducing the surface pressure.

In common, both cases showed similarly large values of cold advection in the lower stratosphere after the passage of a warm anomaly there. This is suggestive of upwind development creating an area of ascent in the lower stratosphere which moved downwind, leading to the increasing values of cold advection observed over C7L. The contribution to the observed deepening of the surface low in this case, due to its translation under increasing thickness values in the atmosphere above 100 hPa, that was calculated for Case 4, was not calculated in Case 5, as in this case the surface low was on a track nearly parallel to the direction of the 100 hPa geopotential

contours in the vicinity of C7L. Also, as mentioned earlier, unlike Case 4, there is some evidence of dynamic development in the lower stratosphere easily sufficient to lower the surface pressure from the 986 hPa observed at 0600 UTC at C7L to the 978 hPa analysed 6 hours later, equivalent to a change of about 7 gpdam in the 1000 hPa geopotential, and when dynamic warming in the order of 20 gpdam in 6 hours was observed near 0600 UTC on the 13th at C7L, at the time of the passage of the lowest pressure there.

Discussion.

It is hoped that the 5 cases presented above will have been sufficient to illustrate some of the important thermal features always present in the lower stratosphere. The use of thickness budget analysis is possibly the simplest method available to reveal how the pressure at the earth's surface reacts and changes in response to variations in the overlying thermal structure. A common feature of the atmosphere at whichever level it is looked at, is that the local pressure, and the surrounding pressure field, is determined by the overlying thermal pattern. In many instances, tropospheric features, whether troughs or ridges, lows or highs are observed to decay in amplitude upwards through the lower stratosphere until a level is reached where they are virtually undetectable. This implies that these features carry with them a thermal signature in the layers directly above them, particularly in the lower stratosphere. It is especially noticeable with short wavelength features, while large planetary scale waves can be seen to extend their influence higher into the stratosphere. The existence of an undisturbed level, in many cases found to be in the stratosphere between 100 hPa and 50 hPa, above which tropospheric disturbances often have no effect, allows the diagnostics of the thermal changes associated with different surface developments to be limited to two principal layers, the whole troposphere, and the lower stratosphere, which at mid-latitudes can be the 100 to 300 hPa layer.

The thermal changes in the two principal layers are seen to contribute in different ways during various stages in the development of surface lows. In many mid-latitude depressions the surface low first develops in a pre-existing tropospheric baroclinic environment, where it is overlain by a strong geopotential gradient in the upper troposphere. Any disturbance that changes the direction of the flow at that level will distort the underlying baroclinic zone, and if this results in advection of the underlying warm thermal towards decreasing values of geopotential in the upper troposphere, or if that geopotential in undergoing change such that its values are falling, as happens under the influence of development of a lower stratospheric warm anomaly, the surface low will deepen. Disturbances in the upper tropospheric geopotential field are always associated with anomalies in the overlying thermal field, thus the whole process can be envisaged as being driven

from above. The origin of the thermal anomalies in the stratosphere has not been addressed in this paper, but there is plenty of scope for them to develop there, with differential sensible heating by radiative means, and dynamically induced anomalies, which can develop in a favourable vorticity environment, or as the result of orographically induced vertical displacements. The important point to emphasise is that the stratosphere is a favourable environment, being dynamically active and having a temperature structure in the vertical that maximises the dynamical effects.

In the cases given above, there is evidentially a balance and interaction taking place between the dynamic and advective changes to the thermal field in the stratosphere, and which are most pronounced in the lower stratosphere. This balance would appear to hold the key as to how and why features in the upper troposphere amplify and decay, with sometimes quite subtle changes in this balance making the difference between the two. It is possible to envisage feedback mechanisms whereby changes in the vorticity pattern brought about by changes in the overlying thermal field, act in such a way as to amplify these changes in the thermal field. The result is, in the atmosphere below, an amplification of a trough or ridge feature, or the conversion of one to the other. It is possible to envisage that advective changes to the thermal field, possibly brought about by an upwind development, may tip the balance between positive and negative feedback, leading to downstream development or decay. As advective changes in the thermal field will often involve different rates across the flow, this in itself can change the shape of the underlying flow and thus the downstream vorticity. Under certain circumstances, the positive feedback element can be expected to be strong enough to result in dramatic changes in lower stratospheric thickness in a short time, often with similarly dramatic effects at the surface.

It has been common practice over the years, and can still sometimes be seen in papers published in the 21st century, for meteorologists to limit their description of mid-latitude surface developments to the troposphere only. It is often stated that a low deepens because of increasing cold advection on its rearward flank, or that an anticyclone builds because of subsidence warming, or that the strength of an upper tropospheric jet stream owes its origin to a strong baroclinic zone in the troposphere. If mentioned at all, the important developments in the upper troposphere which accompany surface developments, are described in terms such as ‘propagating jets’, ‘jet-streaks’, ‘vorticity advection’, terms not incorrect in themselves, but omitting to mention the links that exist between those developments and the superimposed thermal fields, notably those in the lower stratosphere and troposphere, their interaction and modification. Some papers discuss only that part of the atmosphere below 500 hPa, while others consider 300 hPa as an upper limit, but very few attempt to link, or even mention, changes in the stratosphere which accompany most if not all surface developments. HR is a very welcome exception. In all the cases I have examined over a

period of 5 years, surface developments can always be traced back to thermal changes in the stratosphere. The message which I hope will emerge from this paper is that tropospheric developments should be considered as an extension of concurrent changes taking place in the atmosphere above the troposphere.

Over 40 years ago, Patterson and Smebye (1971) found that in many cases, cyclonic development at low levels commences when and where an area of positive vorticity advection in the upper troposphere begins to spread over an area of warm advection in the lower troposphere. In the cases presented here it would appear from the results of the analysis of the thermal changes in the lower stratosphere, that regions of positive vorticity advection can be inferred from the observed changes in the dynamic term of thermal change. However, it would appear that setting the condition that warm advection be located beneath the area of positive vorticity advection is not always observed, at least at the stage of development of the systems in the case histories, although it may have been the situation at an earlier time in their development.

In a more recent paper, Uccellini (1986) found that the development of the QEII storm of September 1978, was marked by the presence of a deepening short-wave trough/jet streak system. He postulated that explosively deepening cyclones are related to the interaction of dynamical and diabatic processes over the entire extent of the troposphere. The link which Uccellini failed to mention is that which exists between upper tropospheric (short-wave) trough, and the warm thermal anomalies that always overlay them in the lower stratosphere. As this paper has tried to show, the strength and position of upper tropospheric jet streams, and their vorticity patterns, is closely tied to the overlying thermal field and its development.

More recently still, Gyakum (1991), investigating the early stages in the development of the QEII storm, found that there was an apparent pre-conditioning of the atmosphere in the 12 hours prior to the rapid intensification, and suggests that explosive intensification of that storm may be understood in terms of the interaction of two separate vorticity maxima, one moving south-eastwards in the upper troposphere, and the other originating along a zone of strong surface frontogenesis further south. Following from this present study, it would appear reasonable to go one stage further back to ascertain the cause of that storm's explosive development, and attempt to determine the origin of the stratospheric warm anomaly which must have been present over the upper tropospheric vorticity maximum which was driving the system, and was creating the frontogenetic conditions also noted by Gyakum. As in other similar cases studied, this lower stratospheric thermal anomaly may well have been in existence for a number of days prior to the development for which it was ultimately responsible.

In common with most other cases of explosive cyclogenesis, the troposphere over the centre

of the surface low cools as the system intensifies, and this can be seen happening even in the 12 hours prior to the rapid intensification of the QEII storm, over the centre of the southernmost surface low. From Gyakum's figures 3, 4, 9 and 10, it can be seen that the 500 to 1000 hPa thickness fell from approximately 574 to 563 gpdam over the low during the 12 hour period up to 00 UTC on the 9th September 1978. As the 1000 hPa geopotential also decreased by 6 gpdam in the same period, the atmosphere above 500 hPa must have warmed by about 17 gpdam over the surface low centre. No doubt, most of this warming occurred in the lower stratosphere, either as advection or adiabatic adjustment, as the pre-existing warm anomaly propagated over the area from the north-west.

Sanders (1986), after studying 48 'bomb' (explosively deepening) developments between 1981 and 1984, concluded that a common factor was the prominent absolute vorticity maximum at 500 hPa, which approached the cyclone during deepening, and which relative to the storm was initially to the north-west of the centre, ending up to the south. He noted that the vorticity maximum pre-existed the surface cyclone in all cases, and that it strengthened during interaction with the surface storm. Although the 500 hPa level which Sanders chose is possibly not ideal, as vorticity amplitudes are generally greater higher up, at 300 hPa for example, his finding would equally apply at 300 hPa, and once again it is pointed out that vorticity maxima are closely associated with the overlying thermal pattern, with changes in vorticity linked to changes in the thermal pattern in the lower stratosphere.

Figure 13. Thickness change over 12 hour periods in the 100 to 300 hPa layer, relative to two surface lows undergoing explosive deepening over the North Atlantic. Data from the Met Office global coarse mesh model.
13a: 25th November 1988 case, 12 hours prior to maximum deepening. 13c : 25th November case, 12 hours during maximum deepening. 13b: 1st January 1989 case, 12 hours prior to maximum deepening. 13d: 1st January 1989 case 12 hours during maximum deepening. Position of surface low centre marked with L*. Units gpdam.

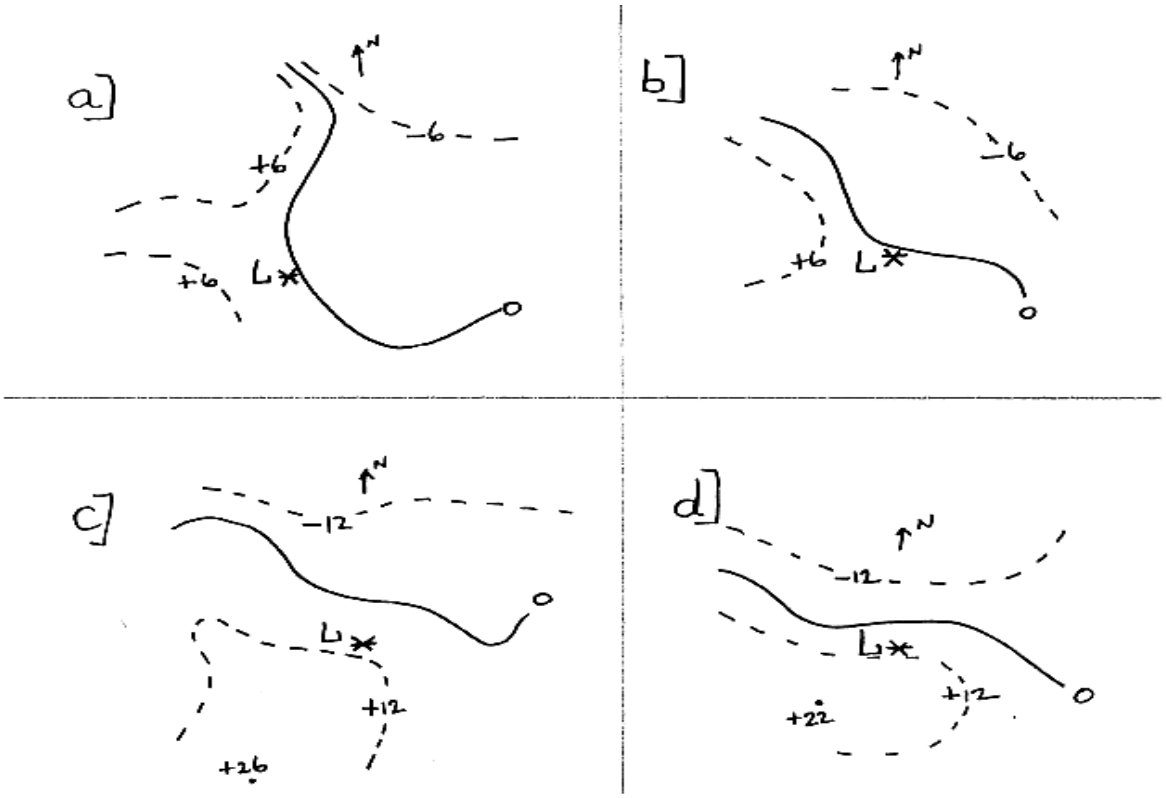

Fig 13

Figure 14. Three examples illustrating the relationship between the 100 to 300 hPa thermal gradient and jet streams at the 300 hPa level. 100 hPa contours, (solid) and 100 to 300 hPa thickness (dashed), units gpdam. 300 hPa wind speed, 80 to 100 knots, shaded, with the inner unshaded region in excess of 100 knots. Data is from the UK global coarse mesh model analysis for 00 UTC on 7th May 1991.

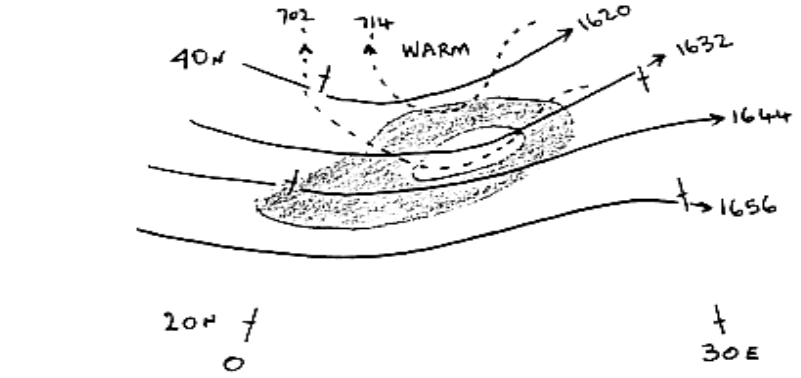

Fig 14a

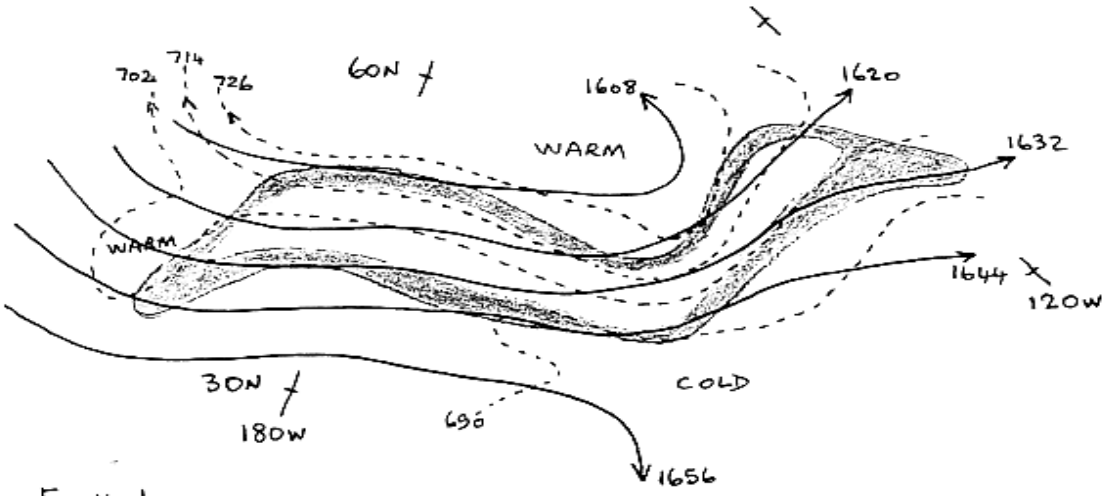

Fig 14b

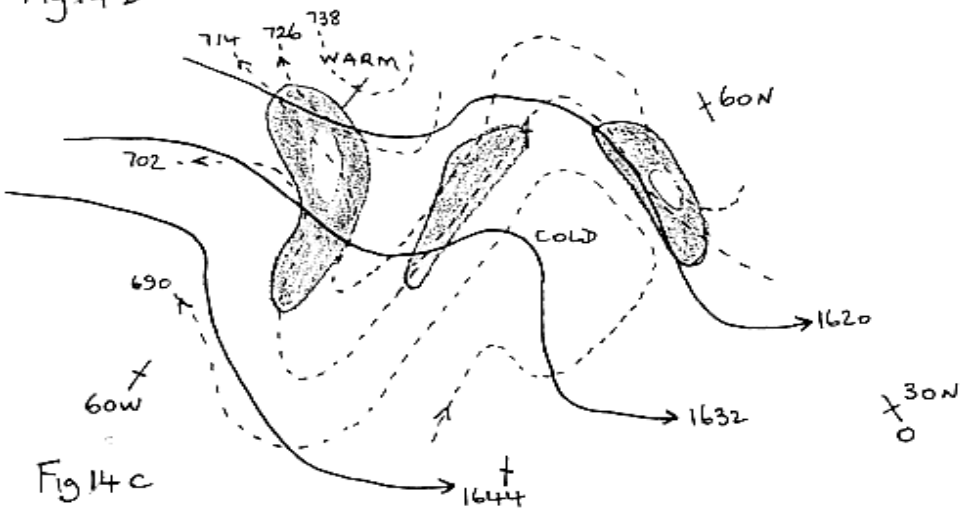

Fig 14c

Although not included in the case studies presented above, two examples using data from the UK Met Office global model output, where the model produced realistic explosive cyclogenesis over the North Atlantic, are briefly mentioned. Figure 13, shows the 12 hour changes in lower stratospheric thickness, (100 to 300 hPa, units gpdam), relative to the low centre. Figures 13a and 13b are the 12 hour changes prior to rapid deepening, 13a for case 1 and 13b for case 2. Figures 13c and 13d are the 12 hour lower stratospheric thickness changes for cases 1 and 2 in the 12 hour period of maximum surface deepening. They illustrates the behaviour of the model's lower stratospheric thickness pattern in two contiguous 12 hours periods prior to and during the maximum deepening stages. The similarity in these two cases is striking, and although it may have occurred by chance, the pattern displayed is fairly common, especially the development of the warm/cold couplet in the lower stratosphere, coincident with rapid intensification of the surface cyclone which is clearly evident. In both cases the surface low was initially located beneath a region of almost zero lower stratospheric thickness change, with thickness decreasing to the north-east and increasing to the west. As the effect of these thickness changes will be to modify the contour pattern at 300 hPa, such that the downwind ridge builds and the upwind trough deepens, the effect over the surface low is to back the flow in the upper troposphere. The knock-on effect on the flow in the mid and lower troposphere will depend on the thermal evolution in the intervening layers, but a backing flow aloft will usually result in a backing flow at mid tropospheric levels also, and it is in this stage of the development the the mid and upper tropospheric flow begins to distort markedly.

In the following 12 hours, Figures 13c and 13d, the period of maximum deepening in both cases , the surface low has migrated south relative to the overlying stratospheric thermal change, such that thickness values have increased by nearly 12 gpdam in the 100 to 300 hPa layer over the low. The cooling/warming dipole has has intensified to the north/south of the low, with increasing thermal changes of similar magnitude but opposite sign. The effect of these thickness changes on the 300 hPa contour field will be to rapidly distort the flow, with strong amplification of the associated trough/ridge couplet, and increases in along flow vorticity gradients. Note the similarity in evolution between the relative movement of the the centres of increasing thickness from west or north-west of the surface low around to the south during the period of rapid surface development, analogous to Sander's finding concerning the absolute vorticity maximum referred to previously. . It is evident fro Figure 13 that this region of the lower stratosphere is very active baroclinically, with considerable tightening of thermal gradients during this period.

Finally, in Figure 14 three examples are given showing the disposition of jet-stream winds, here taken as a gradient of 40 m/s or more, relative to the overlying 100 hPa contour pattern and the

100 to 300 hPa thickness isopleths. For the sake of clarity, contours are drawn at 12 gpdam intervals. Data is from the UK Met Office global analysis for 0000 UTC on the 7th May 1991, the date picked at random, as similar features can be found on any day somewhere around the globe. The examples are from the northern hemisphere. In Figure 14a, the 300 hPa jet can be seen to be made of two principal components. The first is the western lobe of the jet, being a reflection of the overlying 100 hPa flow, which was of similar strength at this time, with a weak thermal gradient in the intervening 100 to 300 hPa layer. The second is the northern lobe which contains the jet maximum, and which is associated with the thermal gradient to the south of a warm anomaly in the 100 to 300 hPa layer. The enhanced flow at 300 hPa is found beneath the region where the warm anomaly protrudes under the region of strength at the 100 hPa level. The 300 hPa jet comes about as a result of the juxtaposing of an easterly thermal beneath a westerly flow. The trough that can be seen in the 100 hPa contours indicates that a warm anomaly was also located in the stratosphere above the 100 hPa level.

In Figure 14b, there is a major 75 m/s plus jet stream located over the Pacific Ocean and as in 14a the jet can be seen to be related both to the 100 hPa flow, which is fairly strong, and to the strong easterly thermal wind in the 100 to 300 hPa layer, on the south side of a large warm zone. Both the jet axis and the various meanders in the jet can be seen to be primarily related to the thermal pattern. Note again that the strength of the jet is derived from a combination of the fairly strong overlying flow at 100 hPa, and the strong 100 to 300 hPa easterly thermal gradient. The warm tongue evident near 160 E is responsible for a trough in the 300 hPa contours at this location, with an associated distortion of the jet on its forward side. A similar but less well developed effect is seen near 150 W, where a warm thermal anomaly produces a trough at 300 hPa, with the associated distortion of the zonal jet there. The overall shape of the jet can be seen to be closely aligned to the lower stratospheric thermal field.

In Figure 14c, there is a highly meridional pattern at 300 hPa, associated with a major Atlantic block, this located under the cold anomaly in the 100 to 300 hPa layer. This example differs from the previous two in the strength of the overlying 100 hPa flow, which in this case is very weak, and which shows some of the characteristics of the meridional flow below, indicating that the thermal anomalies evident in the 100 to 300 hPa layer extended, but to a lesser degree, to the stratospheric layers above 100 hPa. On the periphery of the cold anomaly are two jets, forced by the tightened thermal gradients above them. Upwind a third jet is located under the western side of a warm tongue located above a highly amplified long-wave trough near 50 W. In this example, the shape and location of the jets is clearly a direct reflection of the overlying thermal pattern in the 100 to 300 hPa lower stratospheric layer.

Further Brief Recent Examples

Two more recent examples are presented where there was a substantial change in surface pressure over a few days and at a fixed location. These examples are given because they illustrate clearly the link between changes in surface pressure and changes in thickness in the stratosphere.

To illustrate the type and magnitude of the thermal changes that accompany major changes in surface pressure, thickness values from routine radio-sonde ascents at Herstmonceux (03882), in the SE of England, have been evaluated for selected periods, and the changes in thickness for the following levels ascertained:

1. Above 30 hPa
2. 30 to 100 hPa
3. 100 to 300 hPa
4. 300 to 500 hPa
5. 500 to 1000 hPa

For the purpose of simplicity in this illustration, in the first instance the thickness changes are split between troposphere, up to 300 hPa, and stratosphere, above 300 hPa. 2 cases are for a positive change in surface pressure, and the other 2 are for negative changes. The changes in 3 cases are over a 5 day period, and are for a 6 day period in the remaining case.

Case 1. 23rd to 28th October 2016.
Case 2. 4th to 9th February 2016.
Case 3. 25th to 30th January 2015.
Case 4. 1st to 7th November 2012.

Table 6.

	ΔZ dam Troposphere	ΔZ dam Stratosphere	Start MSLP	End MSLP	ΔP hPa
Case 1	+27	-47	1011	1035	+24
Case 2	-15	+51	1028	986	-42
Case 3	-29	+72	1032	981	-51
Case 4	+28	-68	979	1026	+47

When looking at the thickness changes in Table 6, it needs to be understood that an increase in thickness will lower the pressure below, and a decrease in thickness will raise the pressure below. It is clear that in all these cases the change in tropospheric thickness is in the opposite sense to what would be expected to produce the observed change in surface pressure. When MSLP change was +ve, the tropospheric thickness rose, and vice-versa. But the changes in the region labelled stratosphere are in the correct sense to produce the observed change in surface pressure, and in all cases are of sufficient magnitude to override the tropospheric changes.

From these cases it is clear that on many, probably the majority, of occasions mid-latitude changes in surface pressure are dominated by thermal changes taking place above 300 hPa. One of the reasons for this is that the lower stratosphere is dynamically active, and it is a region with a stably stratified temperature regime. This regime favours quite large changes in temperature for quite modest adiabatic motion. In this respect, the vertical gradient of potential temperature, $d\theta/dp$, is generally much larger in the stratosphere than the troposphere, and the temperature change in a layer that accompany vertical motions where $d\theta/dp$ is large will result in much greater change in mean temperature than where it is small, tending to zero where θ is tending to constant.

Dynamic changes associated with accelerations in the jet-stream region of the troposphere lead to changes in vorticity for the air flowing through the area. Below and above the jet-stream level, along stream vorticity changes generally decrease as they are usually greatest at the level of the maximum wind. Higher in the stratosphere, along stream vorticity changes become less, and often disappear before the mid-stratosphere is reached. This means that the flow undergoes much greater (maximum) vortical stretching and contraction around the jet-stream level, and vanishingly small stretching and contraction higher up.

This stretching and contraction can lead to strong vertical motion in the lower stratosphere, and being a region with a stably stratified temperature regime, to large temperature and thickness changes. A tracer for vertical movement in the atmosphere is isentropic surfaces, which rise and fall alongside the adiabatic changes in which they are embedded. The changes in the vertical separation of isentropic surfaces can also be used as a measure of changes in vorticity, either at a fixed point or along the flow.

The link between changes in the pressure of a fixed isentropic surface with lower stratospheric thickness changes is shown in Figure 16 below. Thickness in the 100 to 300 hPa layer is calculated

while a fixed isentropic surface of 314.6K, in the lower stratosphere, is moved by +/- 80 hPa from a starting value, the temperature at 100 hPa being held constant. The 100 to 300 hPa thickness is seen to change over 55 dam as the isentropic surface ascends and descends.

Fig. 16

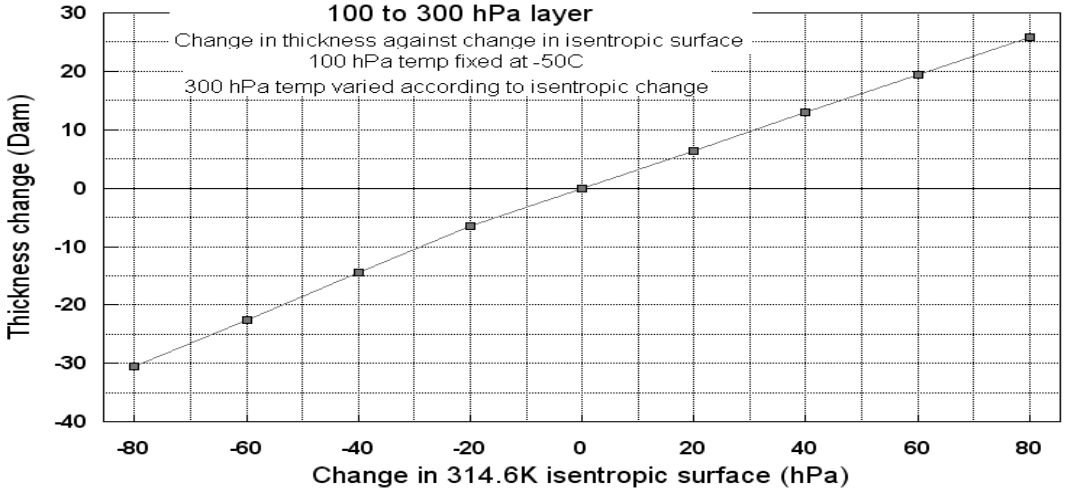

A similar calculation, made by way of illustration, has an initially isothermal temperature of minus 55 C between 100 and 300 hPa. Keeping the temperature at 100 hPa fixed while at the bottom of the layer the air was allowed to descend and ascend adibatically by 50 hPa from 300 hPa. The initial thickness was 701 gpdam, and this fell to 684 gpdam when the base was lifted by 50 hPa, and rose to 715 dpdam when it was depressed by 50 hPa, a change of 31 dam for a total excursion of 100 hPa at the 300 hPa level.

Stratosphere and Mesosphere.

The abnormally low surface pressure over the UK in February 1989, (see case 1 above), would appear to have been caused by a stratospheric warming, not in itself an unusual event, but possibly rare in this case because of the location over which the warming extended. Many researchers have examined these events since they were first observed (Scherhag 1952), and in recent years a rather more complete picture has emerged, following the greater spatial coverage afforded by satellite measurements. Houghton (1978), in a review of middle atmosphere research, presented altitude and longitude cross section of temperature at levels from 0.003 hPa to 10 hPa, around latitude 60N for the 28th/29th December 1976, based on satellite radiance measurements. In the same paper, a chart of the geopotential for the 1 hPa level for the same date was presented, obtained from Labitzke (1977), allowing the calculation of geopotential and thickness around 60N for that day, which was during a period of sudden stratospheric warming. Table 5 shows the thickness values expressed as departures from the zonal mean around 60N on 29th December 1976, for various layers above 10 hPa.

Table 7. Thickness departure from the zonal mean at 60N, for each layer above 10 hPa on 29th December 1976. Units are gpdam.

Layer	Degrees longitude											
hPa	0	30E	60E	90E	120E	150E	180	150W	120W	90W	60W	30W
Above 0.01	-128	-49	-45	-39	-47	0	+99	+145	+168	+92	-66	-129
0.01 to 0.1	-78	-93	-80	-47	0	+36	+41	+92	-91	-78	+24	-64
0.1 to 1.0	+46	+8	+5	-8	-15	-29	-45	-83	-45	+8	+76	+83
1.0 to 10	+166	+139	+95	+62	+4	-56	-120	-191	-188	-114	+35	+163
Net	+6	+5	-25	-32	-58	-50	-25	-37	+26	+64	+69	+53

Table 7 illustrates that in this case in particular, but probably also in general, thermal anomalies of one sign in the mesosphere overlay those of opposite sign in the stratosphere. The layers with the greatest amplitude in the thermal wave are above 0.01 hPa and the 1.0 to 10 hPa layer. The associated atmospheric dynamic waves must be nearly in anti phase too. It should also be noted that there are regions of strong meridional thermal gradient, especially between 90W and 60W, and most marked in the uppermost and lowermost layers. It is near this longitude that the largest net positive thermal anomaly at the base level of 10 hPa is found, indicating that the axis of the resulting 10 hPa geopotential trough is located there too. The amplitude of the zonal thermal wave is in the order of 300 gpdam in the upper mesosphere, and over 350 gpdam in the stratospheric layer 1.0 to 10 hPa. The resulting geopotential wave amplitude at 10 hPa is 127 gpdam.

It is illustrative to examine the average thickness changes between winter and summer that occur in the stratosphere and mesosphere. J.J.Barnett and N.Corney (1985) published tabulated monthly mean zonal values of geopotential, temperature and geostrophic wind for the stratosphere and mesosphere derived from satellite radiance measurements. Their data covers 21 levels between the 137 hPa and 0.006 hPa levels. Using their figures for 60N, it can be seen that the mesosphere is much warmer in winter than in summer, with mean thickness value at 60N in the approximately 6 km thick layer below 82 km 151 dam higher over the months of November, December, January and February, than in the months of May, June, July and August. Comparing the same months lower down in the atmosphere, the difference falls to 6 dam in the 0.125 hPa to 0.340 hPa layer, but increases again in the opposite sense lower still, with the winter 89 dam colder than the summer in the 2.5 hPa to 6.8 hPa level. A table of the thickness values comparison between summer and winter is shown in Table 7.

Table 8. Thickness comparison, winter – summer, for the stratosphere and mesosphere, zonal mean around 60N, based on monthly average values for the levels shown. Thickness values are shown as departures from the annual average. Winter is the mean of the months of November, December, January and February (NDJF), and summer is the mean for the months of May, June, July and August (MJJA). The span and standard deviation (STD) are for 12 months.

Pressure levels hPa	Approx. mid height km	Winter NDJF dam	Summer MJJA dam	Span dam 12 months	STD dam 12 months
0.006 to 0.017	79	+66	-85	175	65
0.017 to 0.046	73	+40	-52	116	40
0.046 to 0.125	67	+17	-18	56	17
0.125 to 0.340	60	0	+6	27	8
0.340 to 0.924	52	-18	+22	54	19
0.924 to 2.51	45	-42	+44	112	38
2.51 to 6.83	38	-40	+49	123	41
6.83 to 18.5	31	-29	+36	91	30
18.5 to 50.4	24	-19	+19	51	17
50.4 to 137	17	-11	+12	27	10

We can clearly see from Table 8 that thickness anomalies of one sign in the mesosphere surmount ones of the opposite sign in the stratosphere. In the winter, when the stratospheric solar heating source is greatly reduced, the coldest levels are centred near 40 km altitude, while the mesosphere above 65 km is warm. In the summer, solar photochemical heating leads to warm layers near 40 km altitude, with levels above 65 km becoming colder. It is evident that there is a level around 60 km where the thickness changes between winter and summer are at a minimum, and the total span, that is the difference between the highest monthly average value and the lowest, falls to 27 gpdam, the same value as is found in the lower stratosphere around 17 km altitude.

The reasons for the vertical temperature structure in the mesosphere, and the associated large thickness changes in the upper mesosphere, are thought to be twofold, a) radiational heat loss b) dynamical effects associated with vertical wave propagation. The second effect is dominant. Through the stratosphere and mesosphere, the amplitude of vertically propagating waves generated by tropospheric disturbances is able to increase due to the conservation of wave energy in decreasing air density. In the upper mesosphere, many of these waves reach an amplitude where they become unstable and break. This imparts a frictional force on the geostrophic flow, allowing cross isobaric movement. The result is a meridional component of flow below the mesopause from the summer pole to the winter one, known as the Dobson/Brewer circulation. This requires general ascending air over the summer pole, and corresponding sinking air over the winter pole, with the associated adiabatic adjustments. Thus, in Table 8, we see the lowest thickness values at the 79 km level in the summer month, and the highest in the winter months.

Further evidence showing the influence that events in the stratosphere can have on the troposphere, as shown in the 25 February 1989 case, is indicated in a diagram by Taylor and Perry (1977). This shows the zonal wind component at various levels from 10 hPa to 1000 hPa, north of 50 N, for the period November 1976 to February 1977, and has been adapted to produce Figure 15. In this figure the departure of zonal mean wind north of 50 N is is shown in units of standard deviation for four levels from 10 hPa to 500 hPa. Fig 15 shows the correspondence between changes in the stratosphere at 10 hPa and those found lower in the atmosphere. There is certainly more than a suggestion that the distinct minimum found near 10 hPa on the 13th January worked its way down through the atmosphere, reaching the 500 hPa layer after 4 days. There is also a similar downward propagation for the maximum near the 2nd January.

Figure 15. Departure of zonal wind north of 50N at at the 10, 100, 300 and 500 hPa levels, in units of standard deviation from the average for the respective levels, over the period 20th December 1976 to 25th January 1977. The diagram has been adapted from one in Taylor and Perry (1977), and illustrates that changes in zonal wind in the stratosphere appear the precede those in the troposphere during that period.

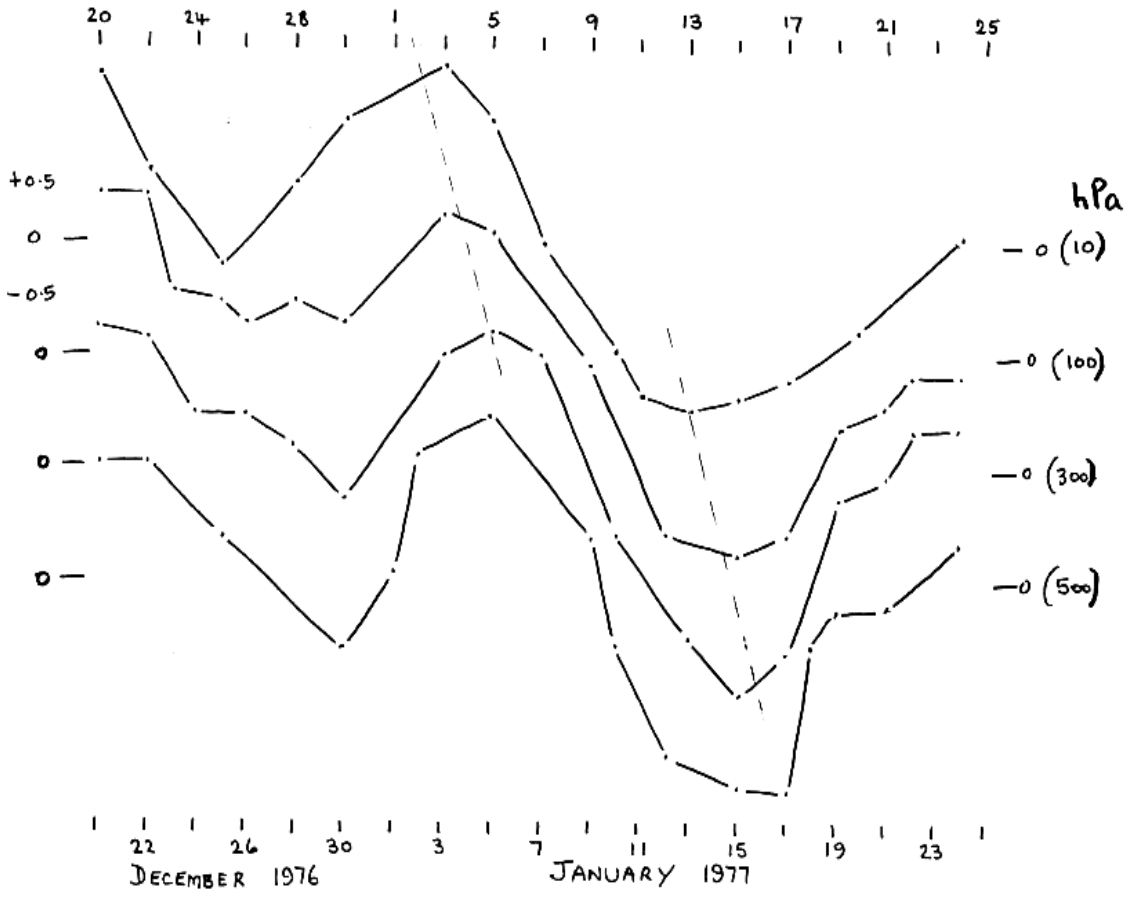

FIG 15

Conclusions.

The five cases presented above were chosen, out of many other similar cases, over a 5 year period, to illustrate the link that exists between the stratosphere and the troposphere, and how changes in one affect the other. From the various investigations carried out the following general conclusions have been drawn up.

a) The geopotential at any point in the atmosphere, (below about 80 km), is determined by just two factors; firstly, the value of the geopotential at some higher point immediately above, and secondly, by the mean temperature of the intervening layer.

b) The geopotential field, and thus the geostrophic wind flow, at any level in the atmosphere, (below about 80 km), is determined by the geopotential field at some level covering the same area immediatly above, and by the intervening thermal field.

c) Any change in the geopotential field at any level in the atmosphere, (up to about 80km), can only occur if either there is a change in the geopotential field at some higher level immediately above, and/or a change in the thermal field of the intervening layer.

d) If the mean temperature in a layer rises/falls, then the pressure, (and geopotential), at the base of the layer will fall/rise relative to the pressure (and geopotential), at the top of the layer. If the pressure at the top of the layer remains unaffected by the change in layer mean temperature, as is usually the case, then the whole effect of the change will be felt at the base.

e) Changes in thickness in a layer are directly proportional to changes in layer mean temperature, and on a synoptic scale, to nothing else. For any layers in the atmosphere, (up to about 80 km), which have the same ratio of top to base pressure, a change in layer mean temperature of the same amount will produce a change in layer thickness also of the same amount.

f) Changes in the thermal field in the stratosphere can arise in three ways, by advection, by adiabatic changes associated with dynamic forcing, and diabatic effects, such as radiation, photochemical, turbulent mixing. Of these advection and adiabatic are the dominant causes of thermal change in the lower stratosphere on the time scale of a day or two.

g) The wind field, and thus the vorticity field, in the upper troposphere, is largely determined by the thermal field in the lower stratosphere. Feedback paths exist such that one can modify the other. Changes in the thermal field can come about by dynamically induced adiabatic changes linked to the vorticity field. These thermal changes can modify the vorticity field resulting in either strengthening of weakening of the dynamically induced changes, causing systems to amplify or decay.

h) Advection of air with differing thermal properties can modify the way in which the vorticity field and thermal field interact. Changes in the thermal gradient, and the resulting changes in the wind field and associated vorticity pattern, can in turn lead to changes in the thermal field which are occurring as a result of adiabatic adjustments resulting from the vorticity pattern.

i) Upwind changes, often dynamically forced, can influence events downwind in such a way as to act as a trigger, which can tip the balance between advection and dynamic changes in a downwind system, so that feedback mechanisms are initiated or existing ones disrupted, with the result that the downwind system may amplify or decay.

Although many surface pressure features owe their existence to the interplay and juxtaposition of various thermal domains acting in the troposphere and lower stratosphere, some features can be traced to events higher in the atmosphere, probably at times even to the mesosphere. As many studies have demonstrated, solar events such as flares, can and do effect the temperature of the upper atmosphere. The suggestion from this study is that any changes to the thermal structure of any part of the atmosphere will have the capability of effecting the layers below. It may be that the path of successful longer range forecasting may be found in a better understanding of the dynamics and thermal structure of the middle atmosphere, and the inclusion of these in global atmospheric models may lead to improved results. (This has indeed been the case in the 25 years since this paper was first drafted).

In many of the cyclonic cases studied, of which the five in this paper are only a selection, an evolution similar to that shown in the HR case was found, where the troposphere was initially relatively warm, but where relative warmth was later found in the lower stratosphere. There does seem to exist, though, another class or other classes of development where either warm tropospheric air is absent, or of very limited vertical extent, or where development ensues under conditions of cooling in both the troposphere and lower stratosphere, in the column above the centre of a surface cyclonic feature. In these cases development of the surface low can be seen to be associated with relative warming at a level much above the lower stratosphere, perhaps as high as the mesosphere in some cases, although evidence of the exact layer or layers responsible for the warming is scanty, as routine data is not normally available much above 10 hPa.

In HR, Part II, it was found that the lower stratosphere descended and warmed above a cold tropospheric dome, and ascended and cooled downstream. This couplet of upwind warming and downwind cooling in the lower stratosphere is a common aspect of nearly all cyclonic developments studied here, and the resulting distortion of the upper tropospheric geopotential field, which is found to intimately linked to the thermal pattern in the lower stratosphere, must be the

primary way in which the tropospheric wind field and thermal pattern are made to evolve.

The conceptional model presented by HR is from the study of a single cyclone. Many of the points in their conceptional model fit the cases shown in this paper, and also fit many other examples not presented, but the initial stage 1 in HR may be rather specific to their case, and other scenarios for the production of an undulation in the tropopause (or a warm anomaly in the lower stratosphere that would be associated with it) may be envisaged. Pertinent here is the possible production of warm anomalies in the middle atmosphere, due either to photochemical processes, or to changes in the solar flux, or associated with the dynamics of wave penetration from the troposphere. Warm anomalies at any level in the atmosphere have the ability to impose a footprint on the atmosphere below, and could initiate short wave features in the upper troposphere.

The occluded stage in HR may also be case specific, as there have been many examples studied here where the development of a surface low did not end when it was under the lower stratospheric warm pool, and in some cases the warm anomaly associated with the cyclonic development at the surface actually passed to the south of the surface low and ended up well to the south-east of it. In other cases, the warm anomaly, after spawning a surface low, continued eastwards to form a subsequent surface low.

Finally, in presenting this paper, and analysing several cases in some detail, an insight may be obtained into the essential role played by the atmosphere above the tropopause in driving the manufacture of much of the weather at the earth's surface. In particular the essential link between the dynamics of the layers above and below the tropopause, especially in connection with the production of mid-latitude cyclones, and also on the generation and modification of the wind flow in the upper troposphere, may be better understood. It is hoped too, that by drawing attention to the use of a simple vertical thermal budget using temporal and/or spatial changes in geopotential thickness, a better understanding of the day to day workings of the atmosphere will be obtained.

Addendum.

In a recent article in the Bulletin of the American Meteorological Society, (BAMS 2012), by H F Dacre, M K Hawcroft, M A Stringer and K I Hodges, data is presented showing the composited structure and evolution of the 200 most intense North Atlantic cyclones from 1989 to 2009.

The data can be found on-line at: www.met.rdg.ac.uk/~storms

This paper is very interesting as it illustrates precisely the fundamental role that thermal changes in the stratosphere have in association with the development of surface pressure features, and in this case, intense North Atlantic cyclones. It also serves to offer further evidence supporting my research in the late 1980's into the links between stratospheric changes and pressure changes at

the earth's surface.

This data set has been adapted to produce figure 17, a composite of the thickness changes occurring in the troposphere and stratosphere over the centre of mean developing cyclone, during the 120 hour period centred on the time of maximum storm intensity (minimum sea level pressure), in 12 hour steps.

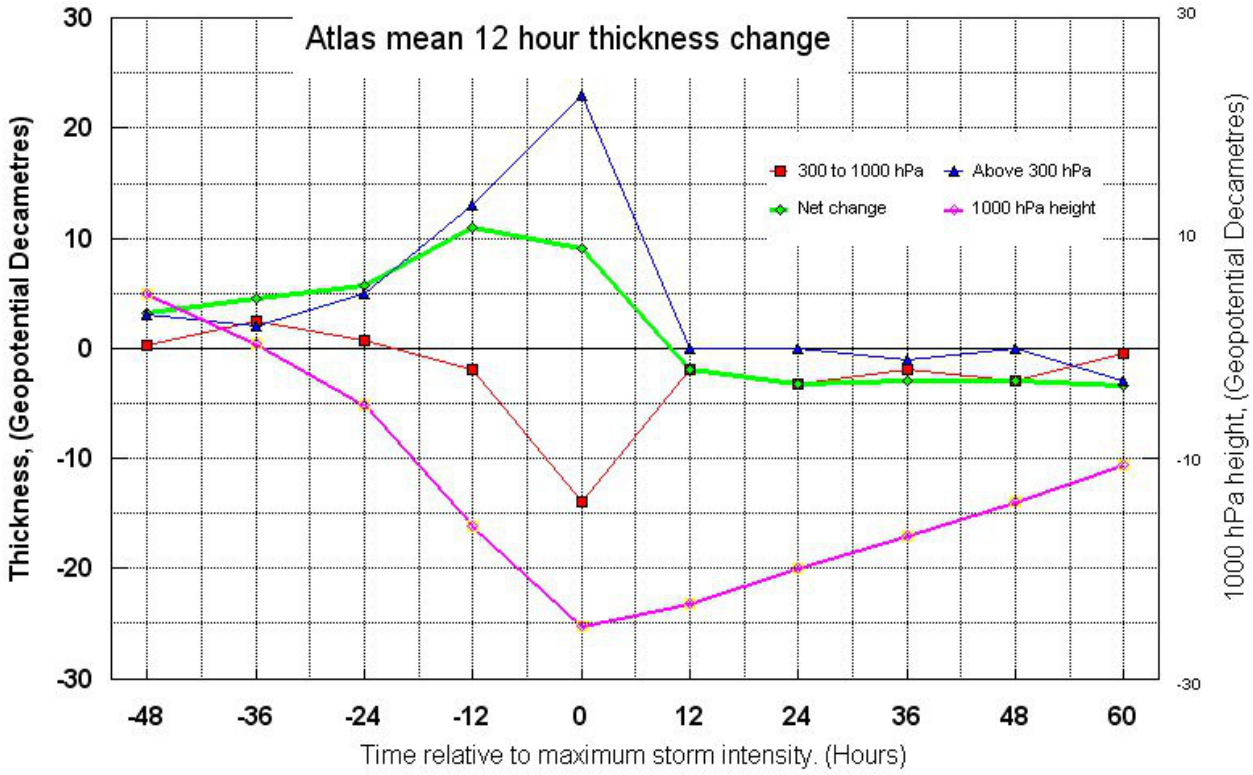

Figure 17. Thickness changes and 1000 hpa height, mean of the 200 most intense North Atlantic cyclones, 1989 to 2007. Blue, thickness changes above 300 hpa, mostly in the lower stratosphere. Red, thickness changes in the troposphere, up to 300 hpa. Green, Net change in the whole atmospheric column. Pink, 1000 hpa height, equivalent to surface pressure.

Initially, in the period T-48 to T-36, when there is a modest fall in 1000 hpa height, stratospheric thickness is increasing slowly, the increase in net thickness and fall in surface pressure being due in equal parts to increasing thickness in the troposphere and stratosphere. From T-36 to T-24, there is a slight increase in the rate of net thickness increase despite the tropospheric change being close to zero, accounted for by a steady increase in stratospheric thickness. Surface pressure has continued to fall at a steady rate. From T-24 to T-12, we see the surface pressure fall accelerate, following the marked upturn in net thickness increase. However, during this interval, the tropospheric thickness change becomes negative, thus cold advection is occurring over the low

centre. The stratospheric thickness change, on the other hand, has increased markedly, and is entirely responsible for the fall in surface pressure, counteracting the cold advection in the troposphere. From T-12 to T0, we see a decrease in net thickness change, though it is still strongly positive. The rate of stratospheric thickness change reaches a maximum value in this period, at the same time the rate of tropospheric thickness change shows that maximum cold advection is occurring there. Surface pressure falls to its lowest value following these changes. From T0 to T+12, for the first time we see the net thickness change move from strong positive to slight negative. This has come about due to the stratospheric change going from very strong positive to zero, at the same time as the tropospheric change goes from strong to slight negative, and the surface pressure over the low centre starts to increase. From T+12 to T+60 the net thickness change remains slightly negative, and as a result the surface pressure rises steadily. Up to T+48 the troposphere continues to cool steadily while the stratosphere remains unchanged. From T+48 to T+60, although the net change remains steady and negative, the stratosphere actually starts to cool in this period, off set by the tropospheric thickness change going from negative to near zero.

B J Burton. FRMetS

November 1993, October 1995, revised November 2018.

References.

Barnet J.J., Corey M. 1985: Middle Atmosphere Reference Model derived from satellite data. Handbook for MAP, V16, p47-85.

Burt, S.D., 1989: London's lowest barometric pressure in 167 years. Weather, 44, 221-225.

Burton, B.J. 1993: Atmospheric pressure, and temperature aloft. Weather, 48, 141-147

Dacre, H.F., Hawcroft, M.K., Stringes , M.A., Hodges, K.I.: Bull AMS, October 2012, 1497.

Hirschberg, P.A. and Fritsch, J.M. 1991: Tropopause undulations and the development of extratropical cyclones, Parts I and II. Mon. Wea. Rev., 119, 496-550.

Houghton, J.T. 1978: The stratosphere and mesosphere. Quart. J. Roy. Meteor. Soc., 104, 1-29

Labitzke, K. Petzoldt, K. Naujokat, B. Klinker, E. Lenshow, R. 1977: Beilage zur Berliner Wetterkarte des Institut fur Meteorologie der freien Universitat, Berlin, 27 January 1977.

Petterson, S. and Smebye, S.J., 1971: On the development of extratropical cyclones. Quart. J. Roy. Meteor. Soc., 97, 457-482.

Sanders, F. 1986: Explosive cyclogenesis in the west-central North Atlantic ocean, 1981-1984, Part I: Composite structure and mean behaviour. Mon. Wea. Rev., 114, 1781-1794.

Sherhag, R. 1952: Die explosion sartigen stratospherenerwarm-ungen des spatwinters 1951-1952. Ber. Deut. Wetterd., 6, 51-63.

Taylor, B.F. and Perry, J.D. 1977:n The major stratospheric warming of 1976-7. Nature, 267, 417-550

Uccellini, L.W. 1986: The possible influence of upstream upper-level baroclinic processes on the development of the QEII storm. Min. Wea. Rev., 114, 1019-1027.